




Taxonomic and palaeobiological implications of a large, pathological sabretooth (Carnivora, Felidae, Machairodontinae) from the Lower Pliocene of South Africa

by CAITLIN RABE^{1,*} , ANUSUYA CHINSAMY¹  and ALBERTO VALENCIANO^{1,2,3,*} 

¹Department of Biological Sciences, University of Cape Town, Private Bag X3, Rhodes Gift, 7701, Cape Town, South Africa; rbxcai002@myuct.ac.za

²Research & Exhibitions Department, Iziko Museums, Cape Town, South Africa

³Departamento de Ciencias de la Tierra and Instituto Universitario de Investigación en Ciencias Ambientales de Aragón (IUCA), Área de Paleontología, Universidad de Zaragoza, C/Pedro Cerbuna, 12, 50009, Zaragoza, Spain; a.valenciano@unizar.es

*Corresponding author

Typescript received 9 February 2022; accepted in revised form 13 May 2022

Abstract: We describe the most complete postcranial remains of a pathological, large-bodied sabretooth from the Lower Pliocene site of Langebaanweg ‘E’ Quarry (South Africa). The skeleton consists of hind limb and vertebral elements that exhibit distinctive exostoses, osteophytes and eburnation. We performed a quantitative morphological comparison of the new postcranial remains found in Langebaanweg, with other Neogene and Quaternary sabretooth and non-sabretooth felids, consisting of the genera *Amphimachairodus*, *Machairodus*, *Lokotunjailurus*, *Dinofelis*, *Panthera*, *Homotherium* and *Smilodon* from several sites in Africa, Europe and North America, using principal component analysis and Mosimann transformations. Although the pathological deformation of the remains distorted some of

the linear measurements, most of the analysed variables do not contain pathological features, and strongly indicate that the Langebaanweg sabretooth is morphologically closer to *Machairodus aphanistus* and *Lokotunjailurus emageritus* than it is to *Amphimachairodus giganteus*. This indicates that the remains could belong to an undetermined sabretooth species from the Langebaanweg locality. The observed pathologies in the foot and lumbar spine are consistent with diagnostic criteria for severe osteoarthritis (due to maturity), which would have limited limb mobility with severe consequences for hunting success.

Key words: South Africa, sabretooth, *Machairodus*, *Lokotunjailurus*, pathology, osteoarthritis.

SABRETOOTH felids are a diverse group with more than 10 well-established genera in the fossil record (Turner 1997; Antón 2013). There are several notable Mio-Pliocene African fossil localities that have yielded sabretooth remains, with the oldest of these being Toros Menalla, an Upper Miocene fossiliferous locality (c. 7–6 Ma) near N’Djamena, the capital of Chad, in Central Africa (de Bonis *et al.* 2010). To date, four sabretooth felids are represented in the fossil record at Toros Menalla: *Amphimachairodus kabir* (Peigné *et al.*, 2005), from TM (Toros Menalla) 266 (type locality) and TM 112, *Lokotunjailurus fononei* de Bonis *et al.*, 2010 from TM 265 (type locality), TM 04 and TM 266, *Megantereon* sp. from TM 166, and *Tchadailurus adei* de Bonis *et al.*, 2018 from TM 112 (Werdelin 2003; Peigné *et al.* 2005; de Bonis *et al.* 2010). Another interesting and diverse Upper Miocene locality is Lothagam in Kenya (Werdelin 2003), where three sabretooth felids are

recorded from the Lower and Upper Nawata Formation (7–5.5 Ma). The most complete is *Lokotunjailurus emageritus* Werdelin, 2003, which represents a large-bodied sabretooth felid that has a mixture of derived and primitive features that obscure its relationship to other African machairodont felids (Werdelin 2003, 2010). Two additional forms, *Dinofelis* sp. and *Metailurus* sp., are also found at Lothagam, although the designation of fossil material to the latter genus is tentative (Werdelin 2003).

There is also a rich diversity of sabretooth felids at the Lower Pliocene site of Langebaanweg ‘E’ Quarry, in South Africa, where at least three different taxa of sabretooths have been found (Hendey 1974a, b; Werdelin 2006): the large Homotherini *Amphimachairodus* Kretzoi, 1929 and two medium-sized Smilodontini, *Metailurus* Zdansky, 1924 and *Dinofelis* Zdansky, 1924. These taxa were first noted by Hendey (1974b), who described the fragmentary remains of two large sabretooths as *Machairodus*

sp. and *Homotherium* sp., as well as assigning a fragmentary maxilla to a new medium-sized sabretooth *Felis obscura* Hendey, 1974b. The original assignment of some of the Langebaanweg material to *Homotherium* Fabrini, 1890 by Hendey (1974b), was subsequently reassessed by Werdelin & Sardella (2006) who provisionally assigned part of the material, consisting of an upper canine (SAM-PQL-11846) and some fragmentary postcranial bones including the calcaneum and astragalus of SAM-PQL-21967 (subadult individual) and the third metatarsal (Mt III) of SAM-PQL-28379 (adult individual), to *Amphimachairodus* sp. They also noted the similarity of this material to the homologous postcranial features of the large machairodont *L. emageritus*. The same year, Werdelin (2006) described the presence of two *Amphimachairodus* taxa at Langebaanweg: *Amphimachairodus* sp. A., consisting of the upper canine SAM-PQL-11846, and *Amphimachairodus* sp. B., which consisted of the postcranial material described by Werdelin & Sardella (2006) that is probably related to *Lokotunjailurus* from Lothagam. Further material described by Hendey (1974b) as *Machairodus* sp., as well as unpublished material housed at SAM (Iziko South African Museum, Cape Town, South Africa) could belong to *Amphimachairodus* sp. B.

Also represented at Langebaanweg is material belonging to *Dinofelis* sp., which was originally assigned to *Machairodus* sp. (Hendey 1974b), and thereafter reassigned to *Dinofelis* sp. by Werdelin & Lewis (2001). Several remains of the Smilodontini, *Dinofelis* and *Megantereon* Croizet & Jobert, 1828, have also been found at younger Pliocene and Pleistocene sites in Africa (Werdelin & Peigné 2010 and references therein). *Dinofelis* is one of the most common extinct felids in the African Neogene, with at least seven documented species (Werdelin & Lewis 2001; Werdelin & Peigné 2010; Madurell-Malapeira *et al.* 2021), which are generally larger than *Metailurus* and range in size from a large lynx to a small lion (Antón 2013). *Metailurus* is known by two species from various African localities (Kenya, Tanzania and South Africa) that date from 6 to 2 Ma (Werdelin & Peigné 2010). Notably, the medium-sized *Felis obscura* has been reassigned into the genus *Metailurus* (Werdelin 2006). The South African material offers rare insight into the postcrania of these genera, which are generally known only from craniodental remains (Werdelin & Lewis 2001).

There are two main goals of this study: (1) to describe and classify new postcranial material of a large sabretooth felid (SAM-PQL-22193 and SAM-PQL-52061) from Langebaanweg E Quarry; and (2) to characterize the pathologies evident in the skeleton and to determine their possible causes and impact on the animal's locomotion and lifestyle.

GEOLOGICAL SETTING

The Langebaanweg (LBW) 'E' Quarry fossil locality forms part of the West Coast Fossil Park (32°58'S, 18°7'E). The site lies *c.* 13 km inland from Saldanha Bay, in the Western Cape province of South Africa (Brumfitt *et al.* 2013; Matthews *et al.* 2015). It is home to world-renowned, rich fossiliferous beds that have provided a wealth of diverse, extinct fauna, representing more than 230 invertebrate and vertebrate taxa including amphibians, marine taxa and small mammals, as well as large giraffids, horses, double-tusked gomphotheres, hyaenids, jackals, felids and the hemicyonid/ursid *Agriotherium africanum* Hendey, 1972 (Hendey 1972, 1974a, b, 1976, 1981a, 1982; Van Dijk 2003; Smith & Haarhoff 2006; Brumfitt *et al.* 2013; Valenciano & Govender 2020a, b; Valenciano *et al.* 2022; Nacarino-Meneses & Chinsamy 2021). Many of the LBW fossil specimens represent the first and/or last appearance of their respective taxa in the fossil record, and the site has been fundamental for a better understanding of the ecology and geology of the Western Cape during the Miocene and Early Pliocene (Franz-Odenaal *et al.* 2002; Matthews *et al.* 2007; Eze & Meadows 2015; Matthews *et al.* 2015).

The sediments that comprise the 'E' Quarry form part of the Varswater Formation (VF), which is part of the larger Sandveld Group (Roberts *et al.* 2011). The members that comprise the VF at 'E' Quarry are the Langeenheid Clayey Sand Member (LCSM), Konings Vlei Gravel Member (KGM), Langeberg Quartz Sand Member (LQSM) and Muishond Fontein Pelletal Phosphorite Member (MPPM) (Roberts *et al.* 2011). The LCSM is the oldest member, dated to the early Middle Miocene, and is overlain by the KVGM, which is dated to the Late Miocene (Roberts & Brink 2002; Roberts *et al.* 2011). Above the KVGM are the dominant fossil-bearing members, the Lower Pliocene LQSM and MPPM (including bed 3aN and 3aS), both dated to 5.15 ± 0.1 Ma (Roberts *et al.* 2011; Valenciano & Govender 2020a). These fossiliferous deposits are aqueous in origin and have been attributed to the deposition of floodplain (LQSM) and riverine (MPPM) sediments (Roberts *et al.* 2011). It has been postulated that the LQSM and MPPM were laid down during a global transgression in the Mio-Pliocene, and there is evidence for this in the occurrence of the VF at *c.* 90 m above sealevel at Elandsfontein farm (Rogers 1980; Hendey 1981b; Roberts & Brink 2002). Although the VF is found only between 30 m and 40 m above sealevel at LBW, this may be due to erosion, suggesting that the sealevel may have reached *c.* 90 m during the Mio-Pliocene deposition of the upper VF fossiliferous layers (Rogers 1980; Roberts & Brink 2002).

PATHOLOGIES IN FELIDS

Palaeopathology is the study of disease and injury in the fossil record, and its study can improve our understanding of the general health, ecology and behaviour of extinct species (Shaw & Ware 2018). For example, pathological conditions of the skeletomuscular elements associated with feeding apparatus and locomotion can give insight into and support for theories regarding hunting behaviour and, subsequently, parental care and sociality (Gonyea 1976; Akersten 1985; McCall *et al.* 2003; Kiffner 2009; Shaw & Ware 2018).

Due to the scarcity of complete specimens of extinct carnivores, studies of pathological individuals are limited and lack standardized definitions (Waldron 2009). Concerning extinct felids, only those from the Late Pleistocene have been analysed in depth (Heald 1989, 1986; Brown *et al.* 2017; Shaw & Ware 2018). Pathologies generally occur relatively infrequently in the carnivore fossil record: Shaw & Ware (2018) noted that only 1% (5100 skeletal elements out of a total of 166 000) of *Smilodon fatalis* Leidy, 1868 specimens in the Hancock Collection from Rancho La Brea (California, USA) had some kind of pathological condition. Furthermore, owing to the lack of standardized definitions, there is often disagreement between researchers on the presence and nature of pathologies. Rothschild & Martin (2011) raised concerns over the misdiagnosis of normal individual variation in skeletal anatomy as pathologies; a result that is likely to be due to studying small sample sizes and fragmentary remains (Rothschild & Martin 2011; Shaw & Ware 2018). There has, however, been some intensive work done on specific collections, such as that completed by Fred Heald (1986, 1989) on the pathology collection at the California State University (Shaw & Ware 2018). Based on 20 years of research into pathologies, Heald developed a scheme of six pathological categories: (1) developmental anomalies; (2) chronic reinjuries; (3) dental disease; (4) traumatic injuries; (5) arthritis; and (6) punctures and/or infections that indicate possible or probable bite wounds (Heald 1989; Shaw & Ware 2018).

Subsequent research on postcranial elements of *S. fatalis* specimens from the Californian Rancho La Brea Museum collection has identified the presence of fractures, bony exostoses, ankylosing spondylitis, osteoarthritis, osteomyelitis, skeletal fusion, hyperostosis, pseudoarthrosis and congenital defects in this species (Shaw & Ware 2018). The oldest record of pathological sabretooth felid remains is a radius of *Promegantereon ogygia* (Kaup, 1832) from the Upper Miocene locality of La Roma 2 in Teruel, Spain (Salesa *et al.* 2014). The specimen shows bony exostoses caused by lesions, and ossification of the tendon of the abductor pollicis longus,

which is an important muscle of the thumb (Salesa *et al.* 2014). Another specimen of *P. ogygia* from a similar age locality (Batallones-1, Madrid, Spain) (Salesa *et al.* 2006) shows a fracture and abnormal healing in a metatarsal. A common pathology in sabretooth felids is bony growths on the humerus, which are often associated with the insertion of the deltoid muscle as seen in both *S. fatalis* specimens from Rancho la Brea, as well as specimens of *Homotherium* from the Senezé and Saint-Vallier localities in France (Ballesio 1963; Argant 2004; Antón 2013). In Africa, there are a number of reports of pathologies in sabretooth felids, although none of these has been comprehensively documented and described. For example, a *Dinofelis* sp. (KNM-ER 4419) from the Upper Burgi Member, c. 2 Ma., Koobi Fora Formation, Kenya (Werdelin & Lewis 2001), shows extensive pathological pitting on various parts of its skeleton (e.g. radius, ulna, calcaneus) and these were interpreted to be due to some form of systemic infection. Another pathology that was briefly noted is that of the bony exostoses on the lumbar vertebrae of a specimen of *Megantereon whitei* (Broom, 1937) from Kromdraai South Africa, which were considered to have occurred as a result of frequent tearing of spinal muscles during struggles with large prey (Antón 2013). Last, Hendey (1974b) observed that pathologies in bones are apparently more common in the Carnivora than in other mammals from Langebaanweg, and recognized osteitis and osteoarthritis in isolated appendicular bones of several specimens of *Machairodus* from the site, similarly to the specimen herein analysed (SAM-PQL-22193).

MATERIAL AND METHOD

Nomenclature and measurements

Anatomical descriptions are based primarily on Evans & De Lahunta (2010, 2013), Ercoli *et al.* (2013, 2015) and Böhmer *et al.* (2020). The terminology conforms to the standard of the Nomina Anatomica Veterinaria (Waibl *et al.* 2005). Measurements were taken using Mitutoyo Absolute digital callipers to the nearest 0.1 mm.

Reporting of the palaeopathologies present in extinct mammal remains is less standardized than for those occurring in hominin remains (Vann & Thomas 2006; De Frans 2010). The pathologies described in this work will be characterized following the operational definitions of skeletal pathologies as defined by Waldron (2009) and with reference to the body of work from Rancho La Brea and others (De Frans 2010; Brown *et al.* 2017; Shaw & Ware 2018; Janssens *et al.* 2019). Pathologies are referred to as mild, medium or severe, following the system of

Bartosiewicz *et al.* (1997) to provide an estimate of relative severity of the pathological impact on the bone element. The term ‘exostosis’ is used to refer to any protrusion of bone from the cortical surface, and pits or pockmarks refer to any minor excavations of the cortical surface (Govender *et al.* 2011; Fernández-Monescillo *et al.* 2019).

Study material

We analysed the unpublished sabretooth felid specimens SAM-PQL-22193 and SAM-PQL-52061 from LBW ‘E’ Quarry (Lower Pliocene, South Africa) housed in the Cenozoic Palaeontology collection of the Iziko South African Museum (ISAM), Cape Town, under the prefix SAM-PQL. The comparative sample includes original postcranial fossils of *Dinofelis* cf. *diastemata* SAM-PQL 20685 from LBW (Hendey 1974b), housed at ISAM, *Amphimachairodus* sp. SAM-PQL-21967 (astragalus and calcaneum) and SAM-PQL-28397 (Mt III) from LBW (Werdelin & Sardella 2006), as well as *Machairodus aphanistus* (Kaup, 1832) from Batallones-1 (Upper Miocene, Spain) housed at MNCN. For comparative purposes we analysed the modern African lion *Panthera leo* Linnaeus, 1758 (SAM-ZM-35042) and leopard *Panthera pardus* Linnaeus, 1758 (SAM-ZM-39998). Additional sabretooth material was analysed using descriptions and measurements from their original publications. A full list of specimens and their associated localities and publications is given in Table S1.

Metrical and multivariate analysis

A set of 57 linear measurements from the vertebrae and hind limb of SAM-PQL-22193 and the calcaneum of SAM-ZM-35042 was taken (Fig. 1; Tables 1, 2). Based on these raw measurements and those of selected felids, we computed four functional indices for the femur and tibia (Table 3), as outlined by Samuels *et al.* (2013). These ratios were used to estimate the proportions of the long bones of the hind limb to make inferences about locomotion. In order to analyse the postcranial skeleton of SAM-PQL-22193 in the context of other medium- and large-sized felids, we performed a principal component analysis (PCA) with PAST 3.0 (Hammer *et al.* 2001), using the linear measurements of a set of 16 variables from the hind limb. This analysis includes variables from the femur (variable 4), tibia (variables 1, 2, 5, 6), calcaneum (variables 1, 2), astragalus (variables 1, 2, 5), metatarsal III (Mt III variables 1, 2) and metatarsal IV (Mt IV variables 1, 2, 3 and 7) (see selected variables in Fig. 1). The PCA is an exploratory analysis of the general structure of a

dataset, which is useful for datasets obtained from the fossil record that are subject to incomplete sampling (Mariani & Romano 2017). As an ordination tool, the PCA reduces the multivariate space to a few independent components that retain much of the variance within a dataset (Jolicoeur & Mosimann 1960; Hammer *et al.* 2001). The sample used for the PCA computation represents the most complete assemblage of measurements that includes *Lokotunjailurus emageritus* and *Amphimachairodus giganteus* Kretzoi, 1929, which are of particular interest to the study due to their morphology and biogeography. The PCA enables exploration of gross morphological variation with a primary focus on sabretooth felids, but also including other felids of similar size, such as the extinct American lion (*Panthera atrox* Leidy, 1853) and the modern African lion (*Panthera leo*). Following previous authors (Meachen-Samuels & Van Valkenburgh 2009; Jojić *et al.* 2014; Ercoli *et al.* 2019; Cuccu *et al.* 2022; Valenciano & Baskin 2022) we calculated the Mosimann shape variables for the raw measurements using geometric mean transformation of data, prior to the PCA (Mosimann & James 1979). The geometric mean is derived from the n th root of the product of n measurements, and the ratio of any measurement to the overall geometric mean is a Mosimann shape variable (Mosimann & James 1979; Meachen-Samuels & Van Valkenburgh 2009).

Performing this transformation corrects the analysis for any isometric effect stemming from different sizes of the sampled material (Ercoli *et al.* 2019). In Figure 2B, where the Mosimann-transformed variables were used, the taxa are plotted differently and can be interpreted without this isometric effect.

RESULTS

The functional indices of the femur and tibia in the selected felids (Table 3) suggest that the sabretooth from LBW has a similar crural index to that of *Amphimachairodus giganteus*, *Machairodus aphanistus*, *Homotherium serum* (Cope, 1893), *Panthera leo* and *P. atrox*. This crural index is smaller than that deduced for *Metailurus parvulus* (Hensel, 1862) but larger than that of *Smilodon fatalis*. According to the femoral robustness index, it also possesses the most robust femora, which is similar only to *P. leo*. Additionally, the LBW sabretooth has a larger femoral epicondylar index than that of *A. giganteus*, but smaller than *Ma. aphanistus*, *S. fatalis*, *H. serum*, *P. leo* and *P. atrox*. It also possesses the highest tibial robustness index, which is comparable to that of *S. fatalis*, *A. giganteus* and *Ma. aphanistus* but contrasts with *Me. parvus*, which has the most slender femora and tibiae of the sample.

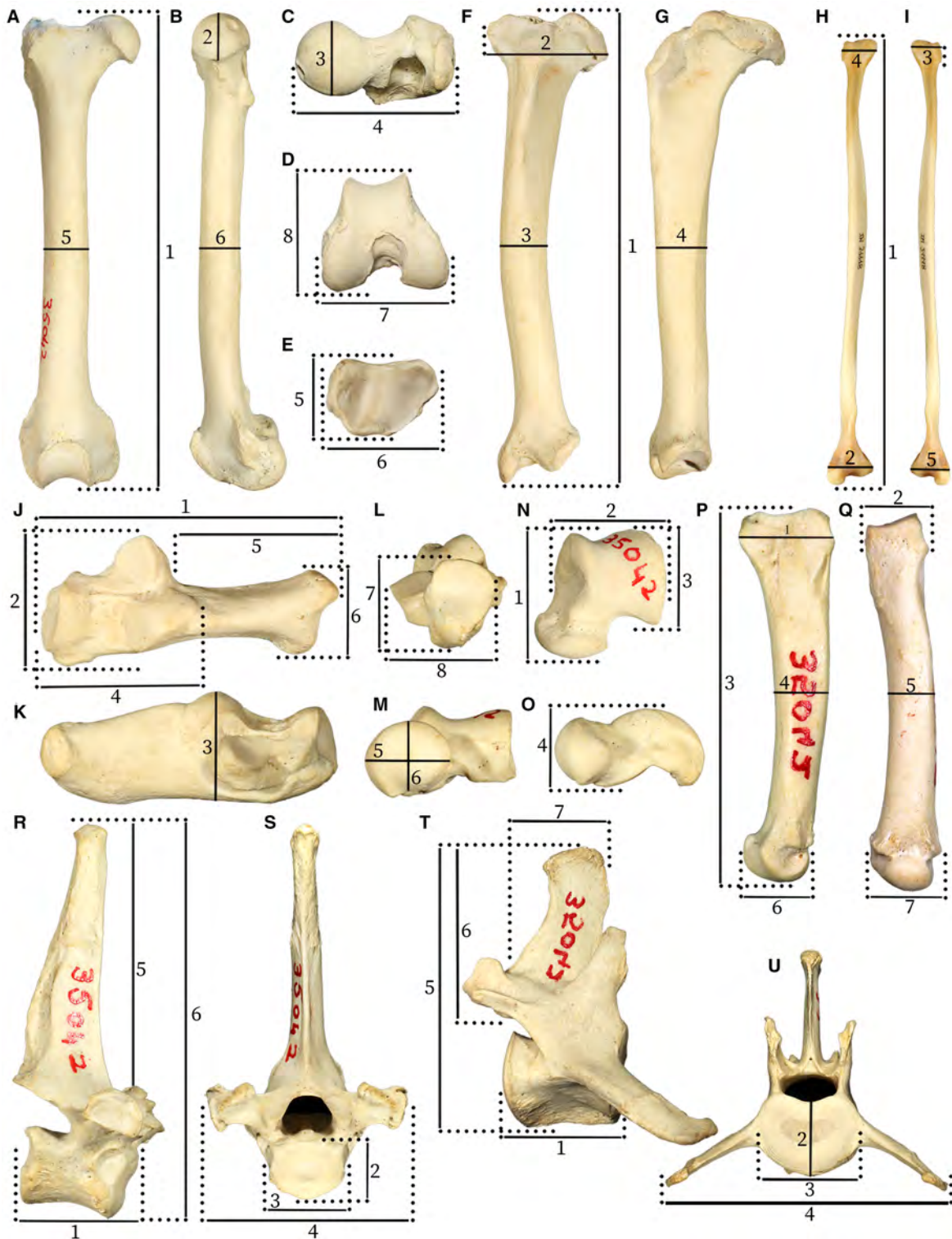


FIG. 1. Postcranial measurements used in this work, illustrated using images of the hind limb and vertebral bones from *Panthera leo* SAM-ZM-35042 and *Panthera pardus* SAM-ZM-39998. A–D, femur in: A, cranial; B, medial; C, proximal; D, distal view. E–G, tibia in: E, distal; F, cranial; G, lateral view. H–I, fibula in: H, cranial; I, lateral view. J–L, calcaneum in: J, dorsal; K, medial; L, anterior view. M–O, astragalus in: N, dorsal; M, anterior; O, lateral view. P–Q, metatarsal in: P, lateral; Q, dorsal view. R–S, thoracic vertebra in: R, lateral; S, cranial view. T–U, lumbar vertebra in: T, lateral; U, caudal view. Descriptions of measurements can be found in Appendix S1.

TABLE 1. Measurements (mm) of the hind limb bones of SAM-PQL22193 from Langebaanweg.

	1	2	3	4	5	6	7	8
Right femur	349	35.3	33.1	86.1	35.2	32.7	70.4	70.3
	367	35.9	32.4	86.0	34.7	32.6	68.7	67.8
	368	37.0	30.5	85.6	35.3	31.9	69.2	68.5
	361.33*	36.09	32.00	85.90	35.03	32.40	69.42	68.83
Left femur	363	36.6	39.3	84.9	33.4	31.4	70.3	64.5
	368	36.8	39.5	83.3	32.7	31.5	70.7	67.8
	368	35.3	39.8	83.3	32.4	31.2	71.9	67.0
	366.33*	36.23	39.55	83.81	32.82	31.39	70.98	66.4
Right tibia	301	73.8	33.8	34.7	37.8	51.6	–	–
	305	73.7	33.2	36.3	38.1	52.3	–	–
	305	72.6	32.5	37.6	37.1	53.9	–	–
	303.67*	73.34	33.16	36.17	37.64	52.58	–	–
Left tibia	297	–	31.8	36.4	41.6	55.0	–	–
	304	–	31.9	35.2	37.8	55.2	–	–
	303	–	31.7	36.1	37.6	53.6	–	–
	301.33*	–	31.77	35.88	39.00	54.59	–	–
Fibula	276	30.8	19.9	31.4	19.3	–	–	–
	274.8	31.1	19.1	30.9	19.7	–	–	–
	274.3	31.1	18.9	31.0	19.9	–	–	–
	275.04*	31.00	19.27	31.08	19.60	–	–	–
Calcaneum	95.5	45.9	43.0	48.0	54.7	30.2	27.3	26.6
	94.5	42.7	39.6	48.9	54.8	30.3	26.8	27.3
	94.8	43.6	41.5	49.0	54.0	30.8	26.3	27.2
	94.93*	44.05	41.34	48.64	54.48	30.43	26.81	27.02
Astragalus	52.1	40.2	40.5	28.7	31.0	21.1	–	–
	51.7	39.8	39.7	28.4	31.0	21.1	–	–
	50.9	40.7	40.2	28.7	31.0	21.2	–	–
	51.55*	40.20	40.14	28.60	31.02	21.12	–	–
Metatarsal II	32.7	19.3	121.4	18.3	12.1	20.8	19.6	–
	33.6	19.1	121.4	17.7	12.1	20.7	19.7	–
	33.9	19.5	121.5	18.4	12.1	20.7	19.6	–
	33.40*	19.30	121.42	18.16	12.10	20.74	19.64	–
Metatarsal III	32.1	23.3	–	–	–	–	–	–
	32.1	23.4	–	–	–	–	–	–
	32.2	23.3	–	–	–	–	–	–
	32.09*	23.33	–	–	–	–	–	–
Metatarsal IV	27.0	22.7	130.6	17.8	14.4	20.5	19.9	–
	27.1	22.4	130.6	15.9	15.2	20.4	20.0	–
	27.0	21.7	130.4	15.9	14.4	20.7	20.0	–
	27.02*	22.26	130.52	16.53	14.65	20.54	19.99	–

Measurements for each fossil element were repeated thrice and rows preceded by an asterisk show the average measurements. See Figure 1A–Q and Appendix S1 for the locations of measurements 1–8.

The eigenvalues (λ), percentages of variance and factor loadings of the Mosimann-transformed variables, obtained from the PCA (Figs 2, 3), are listed in Table 4. We plotted the scores of PC1 against PC2 (Fig. 2B), as well as PC3 against PC4 (Fig. 3). The plot of the first two components of the Mosimann-transformed PCA (Fig. 2B), which account for 92.06% of the total variance in the sample (PC1 = 83.81%; PC2 = 8.25%), shows that there is no overlap between most of the compared species, except for two separate groups of

species that are in close proximity along both components: *P. atrox* (American lion) and *P. leo* (African lion); and *Ma. aphanistus*, *L. emageritus* and the sabretooth SAM-PQL-22193 from the LBW locality. Based on the factor loadings (Table 4), T1 (the length of the tibiae) and Mt IV have the largest loadings of PC1 (loadings of 0.86 and 0.46, respectively), which describes 84% of the variance in the data. This means that a large amount of the variation between the species is explained by the length of the tibiae (T1) and the fourth metatarsals (Mt

TABLE 2. Measurements (mm) of the vertebrae of SAM-PQL22193 from Langebaanweg.

	1	2	3	4	5	6	7
T4	30.0	23.2	27.6	70.1	63.7	110.0	–
	29.5	23.2	27.7	70.0	63.6	110.7	–
	29.5	22.9	27.0	70.3	64.0	110.6	–
	29.65*	23.12	27.42	70.16	63.76	110.42	–
T5–6?	29.7	23.3	29.5	68.7	62.6	105.7	–
	29.2	23.5	29.2	69.1	62.9	103.5	–
	29.1	23.5	29.5	69.2	60.3	103.7	–
	29.29*	23.43	29.41	69.02	61.95	104.29	–
T9	29.2	23.3	30.2	65.6	–	–	–
	29.8	24.1	29.8	65.3	–	–	–
	29.7	23.8	30.4	65.7	–	–	–
	29.57*	23.74	30.13	65.55	–	–	–
T10	30.0	24.8	30.5	–	–	–	–
	29.8	24.7	30.2	–	–	–	–
	29.7	25.1	30.4	–	–	–	–
	29.82*	24.85	30.38	–	–	–	–
T11	–	22.3	30.8	–	39.8	–	–
	–	22.2	30.2	–	40.0	–	–
	–	22.3	30.3	–	42.2	–	–
	–*	22.25	30.42	–	40.67	–	–
T12	29.7	22.9	30.6	66.5	–	–	–
	29.4	23.5	31.0	66.9	–	–	–
	29.4	23.6	30.2	66.9	–	–	–
	29.48*	23.31	30.58	66.75	–	–	–
L2	41.8	29.9	43.3	–	84.2	36.8	32.3
	40.1	29.9	45.8	–	81.9	36.2	32.8
	41.3	29.1	45.8	–	81.9	36.3	33.1
	41.04*	29.65	44.94	–	82.65	36.41	32.72
L4	44.0	30.2	45.5	–	–	–	–
	44.0	32.6	45.4	–	–	–	–
	44.1	32.3	45.1	–	–	–	–
	44.05*	31.72	45.36	–	–	–	–
L5?	–	–	46.4	–	–	–	–
	–	–	47.4	–	–	–	–
	–	–	47.6	–	–	–	–
	–*	–	47.13	–	–	–	–

Measurements for each fossil element were repeated thrice and rows preceded by an asterisk show the average measurements. See Figure 1R–U and Appendix S1 for the locations of measurements 1–7. L, lumbar vertebra; T, thoracic vertebra.

IV 3). T1 and Mt IV 3 also contribute strongly to PC2 (0.43 and -0.55), along with the width of the femoral head (F4) and relative calcaneal length (C1) (0.49 and -0.44 , respectively).

Figure 2B shows that along PC1 the different taxa separate into five groupings: group 1, *Me. parvulus*; group 2, *A. giganteus*, *L. emageritus* and *Ma. aphanistus*; group 3, *H. serum*, sabretooth LBW; group 4, *P. leo* and *P. atrox*; and group 5, *S. fatalis*. Thus, tibial length and Mt IV 3 measurements could be used to separate these taxa. PC2 enables differentiation of *A. giganteus* from the

rest of group 2, and *H. serum* and sabretooth LBW separate from each other. Furthermore, according to Figure 2B, *Me. parvulus*, *L. emageritus*, and *Ma. aphanistus* have proportionally longer calcanea and longer fourth metatarsals, along with *P. leo*, *P. atrox* and the LBW sabretooth. *Smilodon fatalis*, *H. serum* and *A. giganteus* are characterized by a relatively wider proximal epiphysis of the femur.

Consideration of PC3 permits further differentiation of the taxa (Fig. 3). The plot of the third and fourth components of the Mosimann-transformed PCA (Fig. 3) accounts for 5.37% of the total variance in the sample (PC3 = 3.29%; PC4 = 2.08%). Based on the factor loadings (Table 4), it is evident that all of the features appear to contribute to PC3 to a lesser or greater degree, with higher positive loadings for relative calcaneal length (C1), mediolateral width of the astragalar body (A2) and length of the fourth metatarsal (Mt IV 3), as well as Mt IV 2. The mediolateral width of the astragalar body (A2) and calcaneal length (C1) contribute the most to PC4 (0.65 and -0.51 , respectively). Therefore, PC3 and PC4 separate species with relatively long or short calcanea and relatively wider or narrower astragalar bodies. *Metailurus parvulus*, *P. atrox*, *S. fatalis*, *Ma. aphanistus* and *A. giganteus* are all characterized as having relatively longer calcanea and, except for *A. giganteus*, wider bodies of the astragalus, along with *H. serum* and the LBW sabretooth. *Homotherium serum*, *L. emageritus*, *P. leo* and the LBW sabretooth are characterized by relatively longer fourth metatarsals.

Although the plot in Figure 2B shows the LBW sabretooth closer to *Ma. aphanistus* and *L. emageritus*, the plot in Figure 3 shows the differences between the three, with the South African sabretooth having the proportionally longer fourth metatarsal than *L. emageritus*, and *Ma. aphanistus* having the proportionally longest calcanea and widest astragalus of the three. In relation to *A. giganteus*, Fig. 2B indicates that the LBW sabretooth has a longer fourth metatarsal while *A. giganteus* has a longer tibia and wider proximal epiphysis of the femur. Fig. 3 additionally indicates that *A. giganteus* has a proportionally longer calcaneum and wider astragalus.

Institutional abbreviations. AMNH, American Museum of Natural History, New York, USA; AMNH F:AM, Frick Collection of fossil mammals in the AMNH; AMPG, Athens Museum of Palaeontology and Geology, Greece; BPI, Bernard Price Institute University of the Witwatersrand, Johannesburg, South Africa; GPM, George C. Page Museum, Los Angeles, USA; ISAM, Iziko South African Museum, Cape Town, South Africa; LBW, Langebaanweg 'E' Quarry, (South Africa); LGPUT, Laboratory of

TABLE 3. Functional indices from the femur and tibia, based on Samuels *et al.* (2013), of extinct sabretooth felids, large felids and the extant lion.

Taxa	Index			
	Crural	Femoral robustness	Femoral Epicondylar	Tibia robustness
Sabretooth from LBW	84.06	8.91	19.10	10.80
<i>Amphimachairodus giganteus</i>	84.66	7.37	18.29	10.40
<i>Machairodus aphanistus</i>	86.86	7.92	19.97	10.34
<i>Smilodon fatalis</i>	74.41	8.57	21.35	10.75
<i>Panthera atrox</i>	85.85	8.38	21.55	10.06
<i>Homotherium serum</i>	85.15	8.39	20.17	9.61
<i>Metailurus parvulus</i>	96.20	7.22	18.70	7.31
<i>Panthera leo</i>	85.20	8.76	20.92	9.91

All values are based on one individual, except *Machairodus aphanistus* (n = 2), *Smilodon fatalis* (n = 10); *Panthera atrox* (n = 10) and *Homotherium serum* (n = 8), for which the values represent an average of measurements from different individuals. See Tables 1, 2, S1–S5 for raw data and associated references. LBW, Langebaanweg.

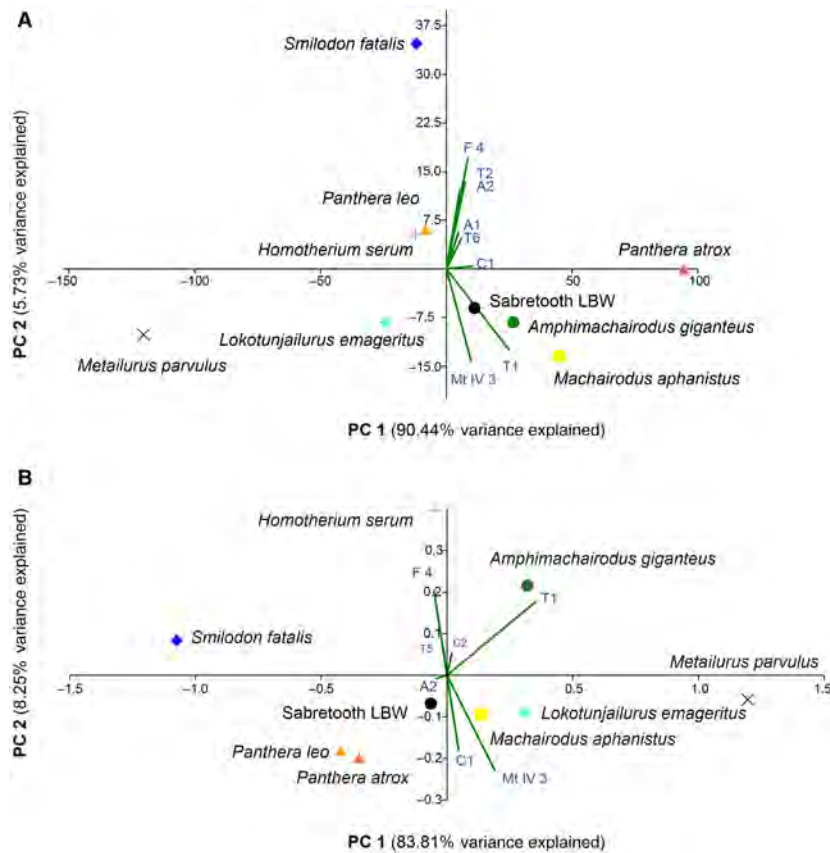


FIG. 2. Plot of the first (PC1) and second (PC2) components of the principal component analysis of the 16 linear measurements taken from a sample of hind limb bones of large felids, consisting of extinct taxa from the Neogene and Quaternary periods as well as the extant African lion (*Panthera leo*). A, raw data. B, Mosimann-transformed data. Abbreviations: A1, 2, astragalus measurements 1, 2; C1, 2, calcaneum measurements 1, 2; F4, femur measurement 4; LBW, Langebaanweg; Mt IV 3, fourth metatarsal measurement 3; T1, 2, 5, 6, tibia measurements 1, 2, 5, 6.

Geology and Palaeontology, University of Thessaloniki, Greece; MNCN, Museo Nacional de Ciencias Naturales, Madrid, Spain; MNHN, Muséum national d'Histoire

naturelle de Paris, France; NHML, Natural History Museum, London, UK; NMB, Naturhistorisches Museum Basel, Switzerland; NMK, National Museums of Kenya,

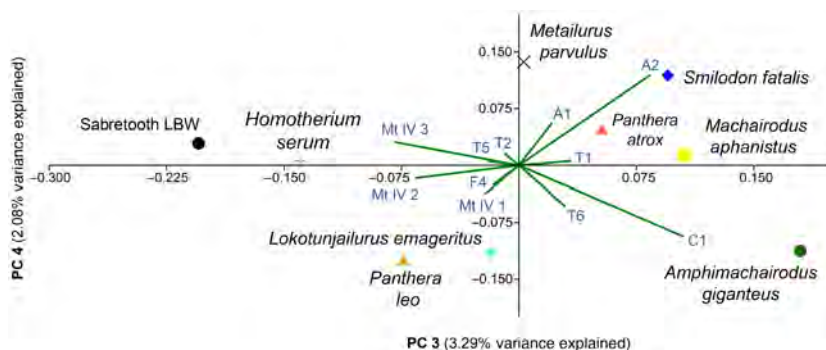


FIG. 3. Plot of the third (PC3) and fourth (PC4) components of the principal component analysis of the Mosimann-transformed variables of 16 linear measurements taken from a sample of hind limb bones of large felids, consisting of extinct taxa from the Neogene and Quaternary periods, as well as the extant African lion (*Panthera leo*). Abbreviations: A1, 2, astragalus measurements 1, 2; C1, calcaneum measurement 1; F4, femur measurement 4; LBW, Langebaanweg; Mt IV 1, 2, 3, fourth metatarsal measurements 1, 2, 3; T1, 2, 5, 6, tibia measurements 1, 2, 5, 6.

TABLE 4. Eigenvalues (λ), percentages of variance, and factor loadings of the linear variables transformed into Mosimann variables obtained from the PCA.

	PC 1	PC 2	PC 3	PC 4
λ	0.39	0.04	0.02	0.01
% variance	83.81	8.26	3.30	2.09
F4 Mos	-0.1258	0.4928	-0.0913	-0.1405
T1 Mos	0.8574	0.4298	0.1826	0.0318
T2 Mos	-0.0726	0.0187	-0.0523	0.0886
T5 Mos	-0.0356	0.1603	-0.1057	0.0288
T6 Mos	-0.0300	0.0753	0.1618	-0.2950
C1 Mos	0.1131	-0.4410	0.5744	-0.5114
C2 Mos	0.0482	0.1330	0.0360	-0.0391
A1 Mos	0.0212	-0.1361	0.1155	0.3054
A2 Mos	-0.1135	-0.0222	0.4580	0.6524
A5 Mos	0.0115	0.0183	0.1304	0.0135
Mt III 1 Mos	-0.0075	0.0010	-0.0371	-0.1237
Mt III 2 Mos	-0.0066	-0.0326	0.1091	0.0559
Mt IV 1 Mos	-0.0055	-0.0140	-0.1170	-0.2033
Mt IV 2 Mos	-0.0289	-0.0175	-0.3618	-0.0922
Mt IV 3 Mos	0.4602	-0.5537	-0.4344	0.1682
Mt IV 7 Mos	-0.0128	-0.0345	0.0186	0.0698

A1, 2, 5, astragalus variables 1, 2, 5; C1, 2, calcaneum variables 1, 2; F4, femur variable 4; Mt III 1, 2, third metatarsal variables 1, 2; MT IV 1, 2, 3, 7, fourth metatarsal variables 1, 2, 3, 7; PC, principal component; PCA, principal component analysis; T1, 2, 5, 6, tibia variables 1, 2, 5, 6.

Nairobi, Kenya; PQL, Quaternary Palaeontology (Langebaanweg), Iziko South African Museum, Cape Town, South Africa; TMM, Texas Memorial Museum, Austin, TX, USA; UCMP, University of California Museum of Paleontology, Berkeley, CA, USA; USNM, National Museum of Natural History, Washington DC, USA; ZM, Zoology Mammals, Iziko South African Museum, Cape Town, South Africa.

SYSTEMATIC PALAEOLOGY

Order CARNIVORA Bowdich, 1821

Family FELIDAE Gray, 1821

Subfamily MACHAIRODONTINAE Gill, 1872

Figures 4–8

Material. SAM-PQL-22193, consists of six thoracic vertebrae, three lumbar vertebrae, two femora, two tibiae, the left fibula, the right astragalus, the left calcaneum and the second, third and fourth metatarsals. SAM-PQL-52061, complete left calcaneum.

Locality. Langebaanweg ‘E’ Quarry. Western Cape province, South Africa.

Age. 5.2 Ma; Late Miocene, Early Pliocene

Description

All of the studied material of SAM-PQL-22193 has a yellow–orange colouration on the surface of the bone that may be due to iron in the depositional environment.

Thoracic vertebrae. The thoracic (T) vertebrae T4 and T5 are well preserved, with only a few minor cracks and abrasions (Fig. 4A, C–E). The vertebral bodies are cranio-caudally and dorsoventrally short. Their ventral surfaces show mild rugosity and have a pronounced ventral crest. The prezygapophyseal and postzygapophyseal facets are ovoid and of the tangential type. The spinous processes are long and they taper, almost evenly, to a rounded point. These processes are slightly caudally inclined, with a more pronounced incline in the T5. The transverse



FIG. 4. Thoracic (T) vertebrae of the Langebaanweg sabretooth, SAM-PQL-22193. A, T4, T5, articulated in lateral view. B, T9–T12, articulated in lateral view. C–E, T5 in: C, cranial; D, caudal; E, ventral view. F–H, T9 in: F, cranial; G, caudal; H, ventral view. Scale bar represents 20 mm.

processes are short and robust, and the mammillary processes are short, acute protuberances from the medial ventral surfaces of the transverse processes.

Thoracic vertebrae T9, T10 and T12 are poorly preserved, and T11 is fragmentary (Fig. 4F–H). The vertebral bodies are like those of T4 and T5 but the ventral

surfaces have greater rugosity and bony growth on the surface of the bone (Fig. 4E, H). The prezygapophyseal and postzygapophyseal facets are ovoid and of the tangential type. The spinous process of T11 is preserved and it is shorter and more caudally inclined than that of T4 and T5. The transverse processes are shorter and more robust

than that of T4 and T5. The mammillary processes are broader but similar in shape to that of T4 and T5.

Lumbar vertebrae. The lumbar (L) vertebrae L2, L4 and L5 are poorly preserved (Fig. 5): the cranial and caudal articular surfaces, spinous processes and transverse processes are either abraded, fragmented, or broken. The postzygapophyseal facets appear to be radial, while the prezygapophyseal facets appear to be tangential.

Pathological description of the lumbar vertebrae. The cranial, caudal and ventral surfaces of the lumbar vertebral bodies have a striated and pockmarked appearance of varying severity (Fig. 5). The ventral surface of L2 has two abnormal, large, bony protuberances on either side of the ventral crest (Fig. 5A, B). The cranial articular surface of the L4 vertebral body has grooves around the circumference (Fig. 5C). The entire vertebral body of L5 is severely eroded and affected by exostoses and osteophytes. The ventral and lateral surface of the body has severe osteophyte growths and there is a pronounced bony spur projecting from the distal cranial surface of the vertebral body (Fig. 5F, G). The cranial surface is flattened and there is eburnation of the entire surface as well as deep pockmarks (Fig. 5E). The central body of the caudal surface has many pockmarks.

Femora. The left femur is well preserved despite the numerous superficial cracks on the cranial and caudal surface of the femoral shaft (Fig. 6A–D, G, H). There is a mediolateral break above the medial supracondylar tuberosity, and the medial part of this crack is restored with a cast. The right femur is less well preserved (Fig. 6E, F). It has numerous superficial, proximodistal cracks. There is a large fracture in the lateral border of the proximal half of the diaphysis. The proximal epiphysis has a transverse mediolateral break on the cranial side, affecting the whole side of the epiphysis. The caudal side of the greater trochanter is also broken. The caudal side of the head and the lesser trochanter show signs of abrasion. A cast replaces a large fragment on the cranial and medial surface of the proximal half of the femoral shaft and a smaller fragment on the caudal side. The lateral and medial supracondylar tuberosities of both femora show signs of abrasion. In medial view the head of the femur is rounded, and the fovea capitis is situated close to the caudal surface. The proximal end of the head lies slightly beneath the tip of the greater trochanter. The neck is mediolaterally short and lies almost horizontal relative to the long axis of the greater trochanter. The greater trochanter is craniocaudally longer than the head. In caudal view the distal part of the greater trochanter forms a pronounced crest along the lateral border of the bone, which extends in a proximodistal manner to the

distal end of the proximal half of the bone. The greater trochanter has two scars for the attachment of the musculi gemelli and the musculi piriformis. The scar for attachment of the m. piriformis runs around the distal cranial surface of the greater trochanter, curving towards the proximal end. The scar for attachment of the m. gemelli lies above that of the m. piriformis and is bounded by pronounced crests. The trochanteric fossa is deep relative to the caudal surface of the bone. The proximal end of the intertrochanteric crest has a slight medial curve. The lesser trochanter is situated on the medial border of the shaft and is substantially projected horizontal to the long axis of the bone. It is more marked and better preserved in the left femur. The diaphysis is straight and has an ovoid section with a transverse diameter slightly larger than that of the craniocaudal. The proximal half of the shaft has an acute lateral border. This is the area for the insertion of the vastus lateralis muscle. The lateral supracondylar tuberosity forms a more pronounced process than the medial one. The patellar trochlea is shallow. The intercondylar fossa is relatively deep compared with the caudal surface of the articular condyles and flares toward the proximal end.

Pathological description of the femora. The left femur has extensive exostosis on the lateral border associated with the attachment area of the m. vastus lateralis (Fig. 6D). Both femora have mild exostoses (i.e. white, calcareous, bony outgrowths) on the lesser trochanter and the proximal and distal ends of the diaphyseal shaft (Fig. 6B). The surfaces of the proximal and distal epiphyses extending onto the diaphyseal shaft have a pitted appearance (series of holes and change in contour of the bone surface) (Fig. 6C).

Tibiae. Both tibiae (Fig. 6I–O) have numerous proximodistal superficial cracks that can be attributed to weathering. The right tibia is generally well preserved, although the tibial tuberosity and part of the craniolateral tibial tubercle are broken. There is some abrasion on the lateral condyle. The proximal half of the cranial border is also broken and has been repaired with plaster. The lateral side of the distal epiphysis of the tibia is broken on the cranial surface. The left tibia is not as well preserved as the right. The lateral side of the proximal end of the left tibia is broken. The proximal epiphysis is broad, and the lateral condyle is slightly larger than the medial one. The proximal part of the lateral condyle lies above that of the medial condyle. The cranial intercondylar area is broader than the caudal, and both are shallow. The intercondylar eminence has two well-defined crests. The tibial tuberosity is not preserved. The tibial crest is preserved and is cranially convex in lateral view. The shaft is robust, sigmoid, and is subtriangular in the proximal half. The



FIG. 5. Lumbar (L) vertebrae of the Langebaanweg sabretooth, SAM-PQL-22193. A–B, L2 in: A, cranial; B, lateral view. C–D, L4 in: C, cranial; D, lateral view. E–G, L5 in: E, cranial; F, lateral; G, ventral view. Scale bar represents 20 mm.



FIG. 6. Long bones of the Langebaanweg sabretooth SAM-PQL-22193. A–D, G–H, left femur in: A, cranial; B, caudal; C, medial; D, lateral; G, proximal; H, distal view. E–F, right femur in: E, cranial; F, caudal view. I–M, right tibia in: I, proximal; J, distal; K, cranial; L, caudal; M, medial view. N–O, left tibia in: N, cranial; O, caudal view. P–R, left fibula in: P, cranial; Q, proximal; R, distal view. Scale bar represents 20 mm.

caudal surface shows marked areas for the attachment of the musculi tibialis caudalis and the musculi flexor digitorum longus. The distal epiphysis has two facets for the articulation of the astragalus. The medial facet is deeper than the lateral facet. The distal part of the medial malleolus lies above that of the lateral malleolus. The groove in the medial malleolus serves as a passage for the tendons of the m. flexor digitorum medialis and m. tibialis caudalis.

Pathological description of the tibiae. Both tibiae have mild to moderate exostoses and pitting on the proximal (Fig. 6I, L) and distal epiphyses, extending onto the diaphyseal shaft (Fig. 6M).

Fibula. The left fibula is well preserved (Fig. 6P–R), but both articular ends have broken off from the shaft and the proximal diaphysis and epiphysis are cracked. The proximal epiphysis is craniocaudally broad and mediolaterally elongated into an acute crest on the cranial side. The shaft has a subtriangular cross-section. The distal epiphysis is also craniocaudally broad but is mediolaterally flattened. The lateral malleolus is proximodistally elongated and elliptical in shape.

Pathological description of the fibula. The distal epiphysis of the fibula is affected by exostoses on all surfaces (Fig. 6P). Part of the distal articular facet for articulation with the tibia appears to be missing and instead the surface of the bone has numerous small pits (Fig. 6P).

Calcaneum. Although pathological, the anatomy of the left calcaneum (Fig. 7) is reasonably well preserved, showing only some proximodistal superficial cracks that can be attributed to weathering of the bone. The calcaneum is robust and the tuber is almost as long craniocaudally as it is mediolaterally. The medial process of the tuber is considerably longer than the lateral process and the two are separated by a broad, relatively flat area. The sustentacular facet is small, ovoid and slightly concave (Fig. 7A–C). Lateral to this facet, the calcaneal canal is a deep, well-delimited groove that extends towards the distal end of the calcaneum. The ectal facet is broad and, although it is convex in its proximal half, it is slightly concave in its distal half. It presents an acute ridge on the lateral side and multiple striations on the surface. The ridge and striations are proximodistal with a slight inclination towards the lateral side. The surface of the facet has a polished texture, presumably from eburnation associated with the articulation of the astragalus (Fig. 7A). Its lateral border is not rounded but has an indentation that is level with the proximal end of the sustentacular facet. In caudal view the lateral side of the

body tapers towards the distal end and a deep fossa is present on the lateral surface. The fossa covers three-quarters of the lateral side of the calcaneum and is bordered by a pronounced lateral projection. The protuberance of the quadratum plantae process is missing.

Pathological description of the calcaneum. The left calcaneum has been severely affected by pathologies. The tuber is extensively affected by exostoses, as is the cranial surface, the lateral border of the body and the astragalar platform (Fig. 7A–C). The medial surface of the sustentacular facet is entirely covered in the outgrowths and, in caudal view, the surface of the body has a distinct abnormal proximodistal protuberance that borders the groove of the sulcus calcaneus (Fig. 7C). The surface of the ectal facet has a highly polished texture and numerous proximodistal grooves (Fig. 7A).

Astragalus. The right astragalus is well preserved (Fig. 8A–F) and shows some orange staining on the dorsal and ventral surface that is probably the result of iron in the depositional environment. The navicular facet is ovoid in distal view and the head is set on a short, transversely wide neck. The sustentacular facet is small and proximodistally elongated. It is convex in its distal half and concave in the proximal. The ectal facet is broad and uniformly concave. The distal surface of the ectal facet has a polished texture, presumably from eburnation associated with the articulation of the calcaneum. The two facets are separated by a deep proximodistal groove that flares toward the proximal end. The trochlea is transversely broad, and the medial border has a strong lateral curve. There is a deep plantar tendinal groove on the proximal corner of the bone.

Pathological description of the astragalus. The ventral surface of the neck, distal surface of the trochlea and both the lateral and medial surfaces of the right astragalus are mildly affected by bony exostoses (Fig. 8B, D). The medial surface of the trochlea and neck have numerous abnormal pits, varied in size, which give the bone a porous texture (Fig. 8A, E). The ectal facet also has a medium degree of eburnation, less severe than that of the calcaneum (Fig. 8B).

Metatarsal II. The left metatarsal II (Fig. 8G, H, K) is well preserved and presents only a few superficial proximodistal cracks, attributable to weathering. There is some orange staining on the dorsal surface, as well as in metatarsal III and IV. The bone is mediolaterally flattened and the shaft has an ovoid section. In dorsal view the shaft has a medial curve in the proximal half. The proximal end elongates dorsoventrally to form the proximal epiphysis. In proximal view the articular surface is



FIG. 7. A–F, left calcaneum of the Langebaanweg sabretooth SAM-PQL-22193 (pathological) in: A, cranial; B, medial; C, caudal; D, lateral; E, proximal; F, distal view. G–L, SAM-PQL-52061 (healthy specimen) in: G, cranial; H, medial; I, caudal; J, lateral; K, proximal; L, distal view. Scale bar represents 20 mm.

asymmetrical with a prominent lateral notch. It is narrow and dorsoventrally long, with a well-delimited, subtriangular proximal facet.

Metatarsal III. The left metatarsal III (Fig. 8G, I, L) has the proximal part well preserved but the distal epiphysis and much of the dorsal surface of the shaft is absent due to breakage. The remaining shaft appears to be straight and robust, with a circular cross-section. The shaft flares dorsoventrally proximal to the sesamoid fossa. In proximal view the articular surface is convex and almost symmetrical, being wide in the dorsal end,

relatively narrow in the ventral and tapering in the mid-section to form a T-shape. The narrow, medial part of the proximal facet has a prominent angular protuberance. The lateral surface has a deep concavity for articulation with metatarsal IV.

Metatarsal IV. The left metatarsal IV is very well preserved (Fig. 8G, J, M) and has only a few superficial proximodistal cracks, attributable to weathering. The shaft is only slightly mediolaterally flattened and is straight, with an oval-shaped cross-section. The proximal end elongates dorsoventrally to form the proximal epiphysis.



FIG. 8. Langebaanweg sabretooth, SAM-PQL-22193. A–F, right astragalus in: A, dorsal; B, ventral; C, distal; D, lateral; E, medial; F, proximal view. G, Mt II, Mt III, Mt IV articulated in dorsal view. H, K, Mt II in: H, medial; K, proximal view. I, L, Mt III in: I, medial; L, proximal view. J, M, Mt IV in: J, medial; M, proximal view. Scale bar represents 20 mm.

In proximal view the articular surface is slightly asymmetrical and tapers ventrally. It is relatively narrow and dorsoventrally long, with a convex facet.

Pathological description of the metatarsals. The metatarsals are mildly affected by pitting on the proximal and distal epiphyses (Fig. 8G, H).

DISCUSSION

Determination of the remains from LBW

The absence of associated dentition in the studied sabretooth material from LBW (SAM-PQL-22193 and SAM-PQL-52061) hinders the taxonomic assignment of these individuals (e.g. Werdelin & Lewis 2001; de Bonis *et al.* 2010; Forasiepi & Carlini 2010; Werdelin & Peigné 2010). Our cursory examination of the long bones of SAM-PQL-22193 suggested that they belong to a large carnivore, distinct from other large carnivores from the LBW locality and that the remains showed pathological features. The large size of the bones and their gross morphology indicated that these specimens belonged to a felid, which precluded their assignment to other carnivoran groups present in LBW, such as the hyaenid *Chasmaportetes australis* (Hendey, 1974b) (Hendey 1974b, 1978a; Werdelin *et al.* 1994), the giant mustelids *Plesiogulo aff. monspessulanus* Viret, 1939 and *Sivaonyx hendeyi* (Morales *et al.*, 2005) (Hendey 1974b, 1978b; Valenciano & Govender 2020a), or the larger sized hemicyonid/ursid *Agriotherium africanum* (see Hendey 1972).

Most of the unpublished postcranial felid bones in the collection from LBW are assigned to the genera *Dinofelis* and *Machairodus* (Werdelin & Sardella 2006). However, some postcranial material is notably larger than others, as represented by SAM-PQL-22193, as well as the additionally sampled material SAM-PQL-21967 and SAM-PQL-28397. Werdelin & Sardella (2006) suggested, based on reconstructed specimen size, that the latter two postcranial specimens be assigned to the largest known craniodental element from the locality: an upper canine tooth that was initially assigned to *Homotherium* by Hendey (1974b) and then re-assigned to *Amphimachairodus* by Werdelin & Sardella. They argued that the specimen showed no diagnostic similarities with *Homotherium*, whereas the canine tooth exhibits traits that align it with other large machairodont species, such as *Amphimachairodus* (Werdelin & Sardella 2006). It is notable, however, that Werdelin & Sardella (2006) mention that the postcranial skeleton of machairodont felids from the Miocene has not yet been studied to the point where the large LBW specimens can be confidently ascribed to *Amphimachairodus*. The material they described, also here examined, SAM-PQL-21967 (astragalus and calcaneum) and SAM-PQL-28397 (Mt III), has general similarities to the homologous elements in *Lokotunjailurus emageritus* from Lothagam Kenya and is generally smaller in size than both the LBW sabretooth and the average measurements from our sample of *Amphimachairodus giganteus*.

Considering the obtained functional indices of the femur and tibia (Table 3), the unidentified sabretooth from LBW SAM-PQL-22193 has similar hind limb bone proportions to the *Homotherini* from the Upper Miocene, *Machairodus aphanistus* and *A. giganteus*, the Pleistocene *Homotherium serum*, and the pantherines *Panthera leo* and *P. atrox*. These felids are generally classified as having a terrestrial locomotion or lifestyle: rarely swimming, climbing or digging (Samuels *et al.* 2013), but the LBW sabretooth has some interesting morphological differences. The crural index (total tibial length divided by femur length \times 100) is an indicator of the relative proportions of the proximal and distal elements of the hind limb (Samuels *et al.* 2013). In a study by Samuels *et al.* (2013), the crural index was not found to differ significantly with different modes of locomotion, and was therefore not suggested as an accurate indicator of locomotion for extinct carnivores. However, given our limited material and the absence of other functional variables, the crural index is used as an exploratory tool to discuss differences in hind limb morphology and the associated locomotion of different taxa. Note that the crural index could not be calculated for *L. emageritus* because of the absence of these functional variables in the fossil record. The most dissimilar taxa in our sample regarding the crural index are *Smilodon fatalis* (74.41), which has a reduced and robust tibia, and the Late Miocene *Metailurus parvulus*, which has a more elongated and slender tibia (96.2). The LBW sabretooth has the second lowest crural index with respect to the sample (84.06) (most like that of *A. giganteus*), indicating that this felid has a more proportionately reduced tibia than most of the other species. The LBW sabretooth possesses the highest value for the femoral robustness index (craniocaudal diameter of the femur divided by the femur length), which specifies the robustness of the femur and its ability to resist bending and shearing stress (Samuels *et al.* 2013). The LBW sabretooth has a larger femoral epicondylar index (FEI; epicondylar breadth of the femur divided by the femur length) than that of *A. giganteus*, but smaller than that of *Ma. aphanistus*. The FEI refers to the relative area available for the origins of the gastrocnemius and soleus muscles used in the extension of the knee and the plantar flexion of the pes (Samuels *et al.* 2013). The FEI was found by Samuels *et al.* (2013) to be a good indicator of locomotor group, and larger values are associated with more robust, strong limbs for digging, climbing and swimming. Last, the LBW form possesses the highest value of the sample for the tibia robustness index (mediolateral diameter of the tibia divided by the tibia length), although it is comparable to that of *S. fatalis*, *A. giganteus* and *Ma. aphanistus*. According to Samuels *et al.* (2013), tibial robusticity is a measure of the bone's ability to

resist bending and shearing stresses. Based on forelimb and hind limb proportions Samuels *et al.* (2013) classified *S. fatalis* and *P. atrox* as terrestrial and *H. serum* as relatively cursorial. The calculated indices compared with the dataset of Samuels *et al.* (2013) suggest that the felid from LBW was like other machairodontines such as *Ma. aphanistus* and *A. giganteus* but that it had a relatively more robust femur and tibia, and therefore was similar to the terrestrial lion *P. leo*. From this sample only *Me. parvulus* has values that deviate significantly, suggesting a potentially more arboreal lifestyle.

The PCA (Figs 2B, 3) and comparative measurements (Table S2) highlight the ways in which the LBW sabretooth differs from other sabretooths in our sample. Compared with the other African, medium-sized sabretooth felids that are present in the LBW record, the postcranial remains of *Dinofelis* cf. *diastemata* (Hendey 1974b) are much smaller than that of SAM-PQL-22193. Additionally, *Metailurus obscurus*, known by a medium-sized maxilla, is much smaller than specimen SAM-PQL-22193. Based on the Mio/Pliocene distribution, it is of particular interest to compare SAM-PQL-22193 with the large, well-known postcranial remains of *Amphimachairodus* (e.g. Harrison 1983; Roussiakis 2002; Sardella & Werdelin 2007; Koufos 2016 and references therein). *Amphimachairodus kabir* has the distinction of being the only documented African species, and is known by a mandible and humerus from the Upper Miocene of Chad (Peigné *et al.* 2005) and, potentially based on dentognathic data, from the Upper Miocene of As Sahabi in Libya (Sardella & Werdelin 2007). Our material is not directly comparable with this African species due to the limited postcranial material of the latter. The felid from LBW differs from the well-known *A. giganteus* from Pikermi (Roussiakis 2002; Koufos 2016) in that it has a shorter tibia, shorter proximal epiphysis of the femur, proportionally shorter calcaneum and relatively more slender astragalus (Figs 2B, 3). It is important to note that the calcaneum of SAM-PQL-22193 is severely affected by erosive and proliferative pathologies, which alter the natural contour of the bone. However, the healthy calcaneal specimen SAM-PQL-52061, referred to herein as the same taxon, indicates that the LBW sabretooth probably did have a slimmer calcaneum than *A. giganteus*. Comparison of the healthy LBW calcaneum with a calcaneum attributed to *Amphimachairodus coloradensis* (AMNH F:AM104726) indicates that *A. coloradensis* has a relatively longer and more slender calcaneal tuber and proximal epiphysis, while the LBW calcaneum has relatively greater total length.

Regarding the qualitative morphology of the tarsals, the LBW felid's astragalus resembles that of *Amphimachairodus* spp. (*Amphimachairodus coloradensis* AMNH F:AM104726 from Edson Local Fauna, upper Hemphillian

(Upper Miocene) of Kansas, USA in Harrison (1983), and *A. giganteus* from Pikermi) more closely than that of *L. emageritus*, but with the former two species having greater total length and breadth in the body of the astragalus. The length of the neck of the LBW sabretooth's astragalus relative to the body is notably shorter than both *A. coloradensis* and *L. emageritus*.

Although the similar overall size and morphological proportions of the form from LBW (Tables 3, S2, S3) suggest that it could be assigned to *Amphimachairodus*, the PCA indicates the opposite. Comparison of the measurements of SAM-PQL-22193 with other African sabretooth material shows that the LBW sabretooth is placed between *P. leo* and the sabretooths *Ma. aphanistus* and *L. emageritus*, and is distant from *A. giganteus* (Fig. 2B). This implies that SAM-PQL-22193 is more similar in morphology and proportions to *Machairodus-Lokotunjailurus* than to *Amphimachairodus*. It is important to mention that the functional indices (Table 3), although relatively homogeneous between the different taxa considered, indicate a similarity between the Langebaanweg form and both the primitive machairodontine *Ma. aphanistus* and the extant *P. leo*. The presence of *Panthera* cf. *leo* in sediments near the Miocene/Pliocene boundary has been reported by Pickford *et al.* (2009) and Miller *et al.* (2010) in Etosha Pan Member, Namibia (Upper Miocene, c. 6 Ma), although the material is limited to the distal part of a radius. These authors did not consider *Lokotunjailurus* in their comparisons, therefore without this comparison the determination of the Etosha specimen may be uncertain. In any case, it could be inferred that *Lokotunjailurus* has body proportions not far from those of *P. leo*, lacking extreme machairodont features, which indicates that it is a cursorial felid (Antón 2003; Werdelin 2003). Due to the absence of dentitions of large non-machairodontine felids in Langebaanweg, and the large temporal gap between the LBW sabretooth and the population of *Ma. aphanistus* (c. 4 Ma), the most plausible hypothesis is that the skeleton of SAM-PQL-22193 could be attributed to *Lokotunjailurus*. The South African sabretooth differs from both *Ma. aphanistus* and *L. emageritus* in having a proportionally longer fourth metatarsal, shorter calcaneum and wider astragalus (Figs 2B, 3). In comparison with a Libyan specimen, 24P102A (of uncertain assignation to *Dinofelis* sp.) (Rook & Sardella 2008), the LBW sabretooth has a relatively longer Mt IV that has greater depth and breadth in the proximal and distal epiphyses, supporting the notion that this LBW specimen is larger than previously recorded *Dinofelis* specimens.

Therefore, besides the differences in the proportions (Fig. 2B) and the overall morphology of the analysed hind limb, the LBW sabretooth is more likely to be closely related to *Ma. aphanistus* and *L. emageritus*, and we

provisionally suggest that it lies between Werdelin & Sardella's *Amphimachairodus* sp. B and *L. emageritus*. This analysis disregards its assignment to *Amphimachairodus* and shows that this material could represent an as yet undetermined form that shares morphological features with other large Miocene sabretooths (Fig. 3). This study supports previous research that has discussed the presence of a '*Machairodus*' sp. form, based on mandible morphology, dentition and scarce postcranial remains, that is distinct from *Amphimachairodus* and intermediate in morphology between *Machairodus* and *Lokotunjailurus* (Werdelin & Sardella 2006; Sardella & Werdelin 2007; Werdelin & Peigné 2010). Thus, our specimen SAM-PQL-22193 can be provisionally described as a large sabretooth felid that, in the absence of clarification from dentognathic remains, could belong to a distinct species of both *Machairodus* and/or *Lokotunjailurus*.

Description and characterization of palaeopathologies

Of the 19 bones attributed to the sabretooth SAM-PQL-22193, 13 show pathologies that vary in form and degree of severity (Fig. 9). These 13 elements indicate pathologies in the region of the lumbar spine, and right and left hind limbs, which present both proliferative and erosive skeletal pathologies suggestive of degenerative bone disease (Waldron 2009; De Frans 2010).

Osteoarthritis. Both femora, both tibiae, the left fibula, left calcaneum, right astragalus, second, third and fourth metatarsals, and the second, fourth and fifth lumbar vertebrae of the SAM-PQL-22193 have osteoarthritic traits as defined by Waldron (2009). Waldron (2009) suggested that superficial pits may be connected to subchondral cysts (another diagnostic characteristic of osteoarthritis) based on studies of the human skeletal system. The distinctive pathological features observed in the calcaneum, namely the severe eburnation and grooves on the ectal facet (Fig. 7A), and the extent to which the surface of the bone is affected by exostoses (Fig. 7A–F), is in line with the descriptions of osteoarthritis (Waldron 2009). The eburnation and grooves of the articular surface of the ectal facet indicate a total loss of articular cartilage at this junction, causing bare bones to grind against one another in the direction of joint movement (Waldron 2009). The ectal facet of the right astragalus also shows eburnation (Fig. 8B), less severe than that of the calcaneum, which suggests that the missing right calcaneum may be in a similar condition to the left.

Intervertebral disc disease. Pitting on the inferior or superior surfaces of the vertebral body is indicative of intervertebral disc disease (Waldron 2009). Based on the extensive

exostoses and pitting as well as on the presence of eburnation on the lumbar vertebrae (Figs 5, 9A), the lumbar spine may have been affected by intervertebral disc disease as well as osteoarthritis (Waldron 2009; De Frans 2010; Govender *et al.* 2011). The cranial articular surface of the L4 vertebral body also has grooves around the circumference (Fig. 5C), suggesting the grinding of bone due to cartilage degeneration (De Frans 2010). The cranial surfaces of the lumbar vertebrae have many pockmarks (Figs 5A, C, E, 9A), which, if they are cystic lesions, could be evidence of subchondral bone cysts (Janssens *et al.* 2019). Further examination of the internal bone structure would need to be performed to support this hypothesis. Future research on this material would benefit from computed tomography scanning, to assess the extent to which the microanatomy of the bone was affected by the pathologies.

Potential causes for pathologies

Osteoarthritis is a degenerative disease of the articular cartilage of joints, which atrophies with disease progression (Waldron 2009). An inflammatory response to the enzymatic breakdown of cartilage causes bone within the joint to produce more bone to repair the damage (Waldron 2009; Janssens *et al.* 2019). This explains the development of osteophytes around the joint margins, such as in the lumbar vertebrae and calcaneum of SAM-PQL-22193. Osteoarthritis is commonly attributed to old age, whereby the cartilage is subjected to repetitive micro-trauma over a long period of time, as opposed to a single major traumatic injury such as a fall or other wound (Greer 1977; Hardie *et al.* 2002; Clarke *et al.* 2005; Clarke & Bennett 2006; Slingerland *et al.* 2011; Bennett *et al.* 2012; Janssens *et al.* 2019). Subchondral bone cysts, which may be indicated by surface pitting, as in the vertebral bodies of the lumbar spine of SAM-PQL-22193, may develop in areas where cartilage has been eroded by trauma or age (Pouders *et al.* 2008; Bennett *et al.* 2012). Most cases of felid osteoarthritis are primary, meaning that there is no recognized underlying cause other than age (Hardie *et al.* 2002; Bennett *et al.* 2012).

Osteoarthritis has been diagnosed in other sabretooth felids such as *Homotherium* (Janssens *et al.* 2019) and *S. fatalis* (Shaw 1989; Shaw & Ware 2018) and in an isolated tibia of ?*Machairodus* from Langebaanweg (SAM-PQL-6388; Hendey 1974b). Janssens *et al.* (2019) examined the fragmented scapula of a *Homotherium* specimen, diagnosing osteoarthritis based on the observation of a bone cyst and osteophyte, the latter of which is less extensive than those seen in the LBW sabretooth. Shermis (1983) identified eburnation and pitting on the femoral head of a subadult *Smilodon* sp. as evidence of osteoarthritis. A study of injury density and frequency in a sample of *S. fatalis* from

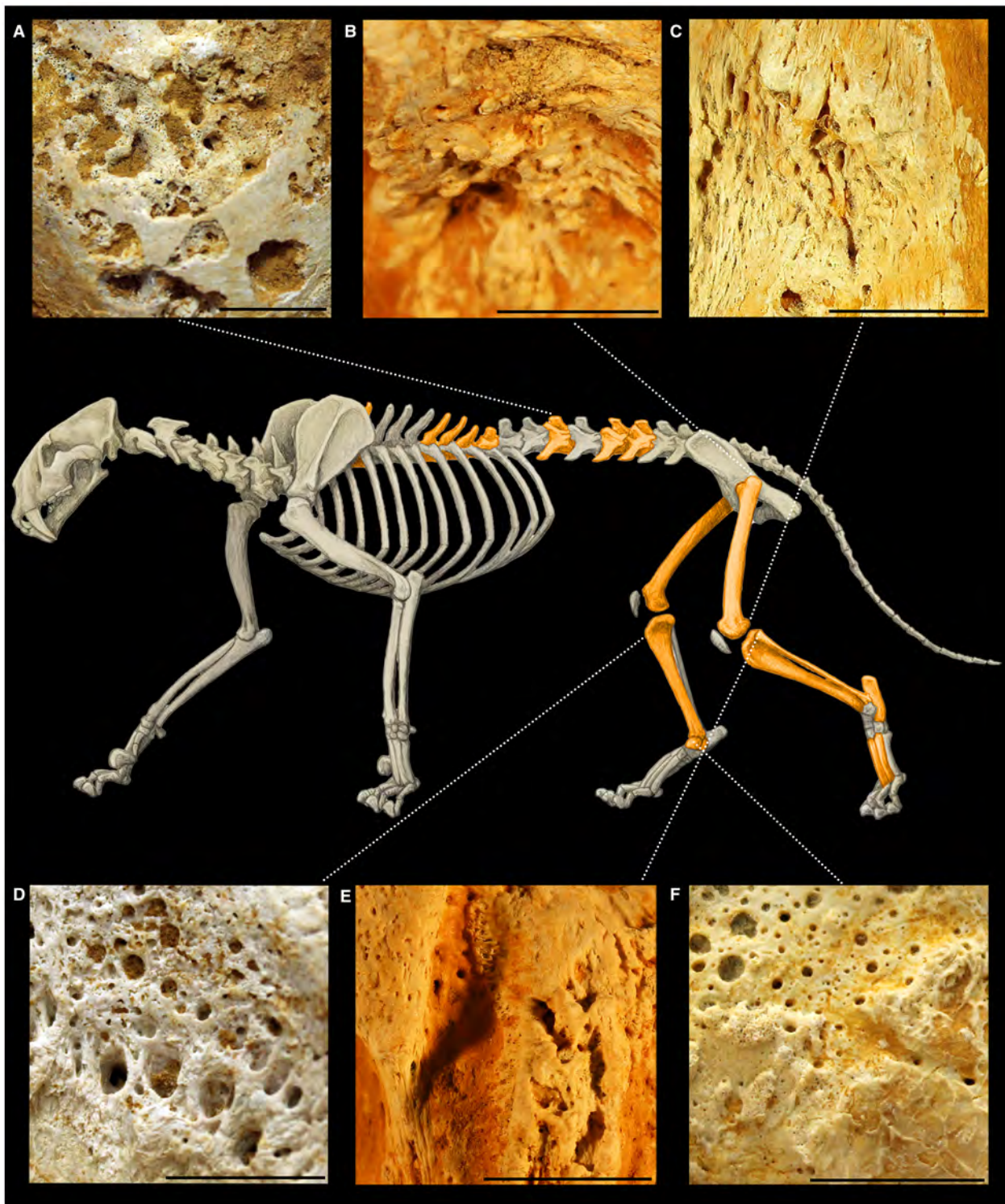


FIG. 9. Diagram of the skeleton of *Amphimachairodus coloradensis* from Antón (2013) highlighting the studied bones of SAM-PQL-22193. A–F, macro images of pathological features: A, pits and erosion on the cranial vertebral body of L2; B, exostoses on the lesser trochanter of the left femur; C, exostoses and pits on the distal diaphyseal shaft of the left femur; D, pits on the proximal epiphysis of the tibia; E, exostoses and pits on the distal epiphysis of the fibula; F, exostoses and pits on the medial surface of the astragalus. Scale bars represent 10 mm.

Rancho la Brea shows an injury hotspot across the entire lumbar region, with 20–50% of all vertebrae showing traumatic pathologies (Brown *et al.* 2017). The osteoarthritic degeneration of the bone was attributed to torsion of the vertebrae relative to one another, as a result of an ambush predation style that puts strain on the lower back when wrestling large prey to the ground (Brown *et al.* 2017). Although the morphology of the LBW sabretooth associates it more with the cursorial Homotherini than the more robust Smilodontini, both groups may have been subjected to lumbar strain and injury when subduing large prey (Antón 2013).

Consequences for locomotion and behaviour

Pathological features in a skeletal assemblage can offer important insights into the life and behaviour of extinct animals (Antón 2013). The sabretooth felid from LBW had severe osteoarthritis of the lumbar spine and left foot, and mild osteoarthritis in the right and left hind limbs. Severe osteoarthritis is known to cause pain in humans and animals, which can limit limb mobility, cause lameness, and result in reduced physical activity (e.g. Lascelles *et al.* 2007; Verruijt 2009 (pp. 10–12); Slingerland *et al.* 2011). Mild osteoarthritis, as observed in domestic cats, can affect locomotive behaviour by reducing mobility and by changing the frequency and height of jumping movements (Clarke & Bennett 2006; Bennett *et al.* 2012). A wild predatory animal with this disease may be unable to hunt effectively and, in social species, this may result in the animal occupying a lower social rank (Sapolsky 2004).

Subordinated individuals may experience additional social and physical stressors through ostracization, caloric deprivation, reduced fecundity and neurological stress (Sapolsky 2004). It is uncertain whether sabretooth felids were social animals (Gonyea 1976; Heald 1989; McCall *et al.* 2003) but current analysis of the nuclear genome and exome of *Homotherium* suggests the presence of genomic adaptations for coordinated social interactions (Barnett *et al.* 2020). Therefore, it is worthwhile to consider the ramifications of impaired mobility for an individual that lives a solitary life as opposed to a social one. Janssens *et al.* (2019) concluded that, in the absence of obvious trauma or infection, the severity of the osteoarthritis in the shoulder of an individual of *Homotherium* indicated that it was a mature individual, and that the condition would be potentially debilitating but not necessarily fatal. Janssens *et al.* (2019) postulated that the degree of degradation must have taken weeks to months to develop and that during that period, the felid must have still been able to hunt or scavenge to survive.

Govender *et al.* (2011), when studying phocid seal remains from LBW, noted that eburnation, as seen on

the calcaneum and lumbar spine of SAM-PQL-22193, is an indication of advanced osteoarthritis. Similarly, De Frans (2010), in his work on camelids, noted that grooves on the surface of vertebral bodies are an indication of advanced and severe cartilage loss. Considering that there is no evidence of trauma in the bones to indicate some kind of injury or septic infection of the joint, and given the advanced stage of the arthritis in the spine and foot, we can hypothesize that the LBW sabretooth developed osteoarthritis due to old age and microwear on the joints, suggesting that the felid was a mature individual. Considering the new findings regarding the probably social behaviour of sabretooths (Barnett *et al.* 2020) it is quite likely that this behaviour may have enabled sick or injured individuals to survive for longer periods of time. Salesa *et al.* 2006 described an abnormally healed fracture of the metatarsals in an individual of *P. ogygia* from Batallones-1, Spain. The authors noted that the survival of the animal for a period long enough for the fracture to heal, and the subsequent limited mobility due to fusion of the bones, suggests that the animal was not entirely self-sufficient (Salesa *et al.* 2006). They concluded that, based on the size of the metatarsals, the individual may have been a young female that was still aided by its mother, as is observed in leopards (Salesa *et al.* 2006). Due to the severity of the disease, the LBW sabretooth would have had considerable pain, which would have impeded movement and hunting ability. It is likely that the felid may have had lameness or difficulty moving the left foot, and it may not have been capable of high mobility to run down prey (McCall *et al.* 2003; Samuels *et al.* 2013).

CONCLUSION

Analysis of the gross morphology and anatomy of the postcranial remains of SAM-PQL-22193 indicates that it was a large-bodied sabretooth felid distinct from other carnivores previously described from the LBW fossil record. The results of a PCA comparing the measurements of SAM-PQL-22193 with other African sabretooth material indicate that the LBW sabretooth is more similar in morphology and proportions to *Machairodus aphanistus* and *Lokotunjailurus emageritus* than to *Amphimachairodus* sp., the largest sabretooth felid described from LBW. Without more diagnostic features from craniodental material we cannot confidently assign this postcranial material to a specific taxon. However, we are confident that our specimen SAM-PQL-22193 is a large sabretooth felid closely related to *Machairodus*–*Lokotunjailurus*, and that it could belong to a distinct species of either genus. Description of the pathologies evident in SAM-PQL-22193 indicate that the sabretooth had severe

osteoarthritis in the hind limbs and that the intervertebral discs in the lumbar region were diseased. The extent and severity of the pathology, in the absence of evidence of a single traumatic event, suggest that the animal developed the condition over time due to repetitive microwear on the joints associated with locomotion and hunting, and old age. The pathology would have caused pain and would have inhibited mobility, suggesting that the animal's long-term survival probably depended on it being a social animal.

Acknowledgements. We thank the following curators and collection managers for access to the material under their care: Dr Romala Govender and Sarena Govender (SAM-PQL), Joffrey Opperman (SAM-ZM) and S. Fraile (MNCN). We also thank J. Samuels (ETSU) for kindly sharing the raw database of postcranial measurements of carnivorans published in Samuels *et al.* (2013). We are especially grateful to Mauricio Antón for allowing the use of his illustration of *Amphimachairodus coloradensis*. GENUS (DSI-NRF CoE-Palaeo) and the Oppenheimer Memorial Trust are acknowledged for financial support for CR for her honours research, and GENUS is acknowledged for the support of AV for his postdoctoral research. Any opinions expressed and conclusions arrived at are those of the authors and are not necessarily to be attributed to GENUS (COE2018-09POST and COE2019-PD07). The NRF African Origins Program (grant number 117716) is thanked for funding support of AC. This paper is also part of R+D+I project PID2020-116220GB-I00, funded by the Agencia Estatal de Investigación of the Spanish Ministry of Science and Innovation (MCIN/AEI/10.13039/501100011033/), the Spanish Ministry of Economy and Competitiveness and FEDER funds (Research Projects PGC2018-094122-B-I00), the Spanish Ministry of Science, Innovation, and Universities ('Juan de la Cierva Formación', ref. FJC2018-036669-I for AV), E33_20R (Gobierno de Aragón), and the Research Group UCM 910607. We are indebted to the editor Mary Silcox and the reviewers Dr H. Gregory McDonald and a second, anonymous, reviewer for their useful comments and suggestions which improved the original manuscript.

Author contributions. AV developed the initial concept for the research. CR and AV performed the data collection and analysis and wrote the first draft of the manuscript. AC assisted and reviewed the manuscript. CR, AC and AV read and contributed to the final draft.

Editor. Mary Silcox

SUPPORTING INFORMATION

Additional Supporting Information can be found online (<https://doi.org/10.1002/spp2.1463>):

Appendix S1. Description of the measurements taken and Tables S1–S5.

Table S1. Additional material used in this study, the associated specimen number, locality, current housing and publication from which descriptions/measurements were referenced.

Table S2. Measurements (mm) of the hind limb bones of large sabretooth species from different localities.

Table S3. Measurements (mm) of the foot bones of large sabretooth species from different localities.

Table S4. Measurements (mm) of the hind limb bones of the extant African lion *Panthera leo* (SAM-ZM-35042), as outlined in Figure 1.

Table S5. Measurements (mm) of the vertebral bones of the extant African lion *Panthera leo* (SAM-ZM-35042), as outlined in Figure 1.

REFERENCES

- AKERSTEN, W. A. 1985. Canine function in Smilodon (Mammalia; Felidae; Machairodontinae). *Contributions in Science*, Natural History Museum of Los Angeles County, **356**, 1–22.
- ANTÓN, M. 2003. Appendix: notes on the reconstructions of fossil vertebrates from Lothagam. 661–665. In LEAKEY, M. and HARRIS, J. (eds) *Lothagam: The dawn of humanity in Eastern Africa*. Columbia University Press.
- ANTÓN, M. 2013. *Sabertooth*. Indiana University Press.
- ARGANT, A. 2004. Les Carnivores du gisement Pliocène final de Saint-Vallier (Drôme, France). *Geobios*, **37**, S133–S182.
- BALLESIO, R. 1963. Monographie d'un *Machairodus* du gisement villafranchien de Senèze: *Homotherium crenatidens* Fabrini. *Travaux du Laboratoire de géologie de la Faculté des sciences de Lyon, New Series*, **9**, 129 pp.
- BARNETT, R., WESTBURY, M. V., SANDOVAL-VELASCO, M., VIEIRA, F. G., JEON, S., ZAZULA, G., MARTIN, M. D., HO, S. Y., MATHER, N., GOPALAKRISHNAN, S. and RAMOS-MADRIGAL, J. 2020. Genomic adaptations and evolutionary history of the extinct scimitar-toothed cat, *Homotherium latidens*. *Current Biology*, **30**, 5018–5025.
- BARTOSIEWICZ, L., VAN NEER, W. and LENTACKER, A. 1997. *Draught cattle: Their osteological identification and history*. Annales-Musee Royal de l'Afrique Centrale, Sciences Zoologiques, Belgium.
- BENNETT, D., MARIAM, S., ARIFFIN, Z. and JOHNSTON, P. 2012. Osteoarthritis in the cat 1. How common is it and how easy is it to recognize. *Journal of Feline Medicine & Surgery*, **14**, 65–75.
- BÖHMNER, C., THEIL, J. C., FABRE, A. C. and HERREL, A. 2020. *Atlas of terrestrial mammal limbs*. CRC Press.
- BOWDICH, T. E. 1821. *An analysis of the natural classifications of Mammalia, for the use of students and travellers*. J. Smith, Paris.
- BROOM, R. 1937. On some new fossil mammals from limestone caves of the Transvaal. *South African Journal of Science*, **33**, 750–769.
- BROWN, C., BALISI, M., SHAW, C. A. and VAN VALKENBURGH, B. 2017. Skeletal trauma reflects hunting behaviour in extinct sabre-tooth cats and dire wolves. *Nature Ecology & Evolution*, **1** (5), 0131.

- BRUMFITT, I. M., CHINSAMY, A. and COMPTON, J. S. 2013. Depositional environment and bone diagenesis of the Mio/Pliocene bonebed, South Africa. *South African Journal of Geology*, **116**, 241–258.
- CLARKE, S. P. and BENNETT, D. 2006. Feline osteoarthritis: a prospective study of 28 cases. *Journal of Small Animal Practice*, **47**, 439–445.
- CLARKE, S. P., MELLOR, D., CLEMENTS, D. N., GEMMILL, T., FARRELL, M., CARMICHAEL, S. and BENNETT, D. 2005. Prevalence of radiographic signs of degenerative joint disease in a hospital population of cats. *Veterinary Record*, **157**, 793–799.
- COPE, E. D. 1893. A new Pleistocene sabre-tooth. *The American Naturalist*, **27**, 896–897.
- CROIZET, J. B. and JOBERT, A. C. G. 1828. *Recherches sur les ossements fossiles du département du Puy-de-Dôme*. Principaux Libraires, Paris, 224 pp.
- CUCCU, A., VALENCIANO, A., AZANZA, B. and DE MIGUEL, D. 2022. A new lynx mandible from the Early Pleistocene of Spain (La Puebla de Valverde, Teruel) and a taxonomical multivariate approach of medium-sized felids. *Historical Biology*. <https://doi.org/10.1080/08912963.2021.2024181>
- DE BONIS, L., PEIGNÉ, S., MACKAYE, H. T., LIKIUS, A., VIGNAUD, P. and BRUNET, M. 2010. New sabretoothed cats in the Late Miocene of Toros Menalla (Chad). *Comptes Rendus Palevol*, **9**, 221–227.
- DE BONIS, L., PEIGNÉ, S., MACKAYE, H. T., LIKIUS, A., VIGNAUD, P. and BRUNET, M. 2018. New sabretoothed Felidae (Carnivora, Mammalia) in the hominid-bearing sites of Toros Menalla (late Miocene, Chad). *Geodiversitas*, **40**, 69–86.
- DE FRANS, S. D. 2010. Paleopathology and health of native and introduced animals on southern Peruvian and Bolivian Spanish colonial sites. *International Journal of Osteoarchaeology*, **20**, 508–524.
- ERCOLI, M. D., ECHARRI, S., BUSKER, F., ÁLVAREZ, A., MORALES, M. M. and TURAZZINI, G. F. 2013. The functional and phylogenetic implications of the myology of the lumbar region, tail, and hindlimb of the lesser grison (*Galictis cuja*). *Journal of Mammalian Evolution*, **20**, 309–336.
- ERCOLI, M. D., ÁLVAREZ, A., STEFANINI, M. I., BUSKER, F. and MORALES, M. M. 2015. Muscular anatomy of the forelimbs of the Lesser Grison (*Galictis cuja*), and a functional and phylogenetic overview of Mustelidae and other caniformia. *Journal of Mammalian Evolution*, **22**, 57–91.
- ERCOLI, M. D., RAMÍREZ, M. A., MORALES, M. M., ÁLVAREZ, A. and CANDELA, A. M. 2019. First record of Carnivora (Puma lineage, Felidae) in the Uquía Formation (Late Pliocene–Early Pleistocene, NW Argentina) and its significance in the Great American biotic interchange. *Ameghiniana*, **56**, 195–212.
- EVANS, H. E. and DE LAHUNTA, A. 2010. *Miller's guide to the dissection of the dog*, Fourth edition. W. B. Saunders Company.
- EVANS, H. E. and DE LAHUNTA, A. 2013. *Miller's anatomy of the dog*. Elsevier Health Sciences.
- EZE, P. N. and MEADOWS, M. E. 2015. Geochemistry and palaeoclimatic reconstruction of a palaeosol sequence at Langebaanweg, South Africa. *Quaternary International*, **376**, 75–83.
- FABRINI, E. 1890. I *Machairodus* (Meganthereon) del Val d'Arno superior. *Bollettino Comitato Geologico d'Italia*, **21**, 121–144.
- FERNÁNDEZ-MONESCILLO, M., ANTOINE, P. O., QUISPE, B. M., MÜNCH, P., FLORES, R. A., MARIVAUX, L. and PUJOS, F. 2019. Multiple skeletal and dental pathologies in a late Miocene mesotheriid (Mammalia, Notoungulata) from the Altiplano of Bolivia: palaeoecological inferences. *Palaeogeography, Palaeoclimatology, Palaeoecology*, **534**, 109297.
- FORASIEPI, A. M. and CARLINI, A. A. 2010. A new thylacosmilid (Mammalia, Metatheria, Sparassodonta) from the Miocene of Patagonia, Argentina. *Zootaxa*, **2552**, 55–68.
- FRANZ-ODENDAAL, T. A., LEE-THORP, J. A. and CHINSAMY, A. 2002. New evidence for the lack of C4 grassland expansions during the early Pliocene at Langebaanweg, South Africa. *Paleobiology*, **28**, 378–388.
- GILL, T. 1872. Arrangement of the families of mammals with analytical tables. *Smithsonian Miscellaneous Collections*, **11**, 1–98.
- GONYEA, W. J. 1976. Behavioral implications of sabretoothed felid morphology. *Paleobiology*, **2**, 332–342.
- GOVENDER, R., AVERY, G. and CHINSAMY, A. 2011. Pathologies in the early Pliocene phocid seals from Langebaanweg, South Africa. *South African Journal of Science*, **107**, 1–6.
- GRAY, J. E. 1821. On the natural arrangement of vertebrate animals. *London Medical Repository Monthly Journal and Review*, **15**, 296–310.
- GREER, M. 1977. Osteoarthritis in selected wild mammals. *Proceedings of the Oklahoma Academy of Science*, **57**, 39–43.
- HAMMER, Ø., HARPER, D. A. and RYAN, P. D. 2001. PAST: paleontological statistics software package for education and data analysis. *Palaeontologia Electronica*, **4** (1), 9.
- HARDIE, E. M., ROE, S. C. and MARTIN, F. R. 2002. Radiographic evidence of degenerative joint disease in geriatric cats: 100 cases (1994–1997). *Journal of the American Veterinary Medical Association*, **220**, 628–632.
- HARRISON, J. A. 1983. The Carnivora of the Edson local fauna (late Hemphillian), Kansas. *Smithsonian Contributions to Paleobiology*, **54**, 1–42.
- HEALD, F. P. 1986. Paleopathology at Rancho La Brea. *Anthroquest*, **36**, 6–7.
- HEALD, F. 1989. Injuries and diseases in *Smilodon californicus*. *Journal of Vertebrate Paleontology*, **9**, 24A.
- HENDEY, Q. B. 1972. A Pliocene ursid from South Africa. *Annals of the South African Museum*, **59**, 115–132.
- HENDEY, Q. B. 1974a. Faunal dating of the late Cenozoic of Southern Africa, with special reference to the Carnivora. *Quaternary Research*, **4**, 149–161.
- HENDEY, Q. B. 1974b. The late Cenozoic Carnivora of the South-Western Cape Province. *Annals of the South African Museum*, **63**, 1–369.
- HENDEY, Q. B. 1976. The Pliocene fossil occurrences in E Quarry, Langebaanweg, South Africa. *Annals of the South African Museum*, **69**, 215–247.

- HENDEY, Q. B. 1978a. Late Tertiary Hyaenidae from Langebaanweg, South Africa, and their relevance to the phylogeny of the family. *Annals of the South African Museum*, **76**, 265–297.
- HENDEY, Q. B. 1978b. Late Tertiary Mustelidae (Mammalia, Carnivora) from Langebaanweg, South Africa. *Annals of the South African Museum*, **76**, 329–357.
- HENDEY, Q. B. 1981a. Palaeoecology of the late Tertiary fossil occurrences in ‘E’ Quarry, Langebaanweg, South Africa, and a reinterpretation of their geological context. *Annals of the South African Museum*, **84**, 1–104.
- HENDEY, Q. B. 1981b. Geological succession at Langebaanweg, Cape Province, and global events of the late Tertiary. *South African Journal of Science*, **77**, 33–38.
- HENDEY, Q. B. 1982. *Langebaanweg: A record of the past*. Rustica Press, Cape Town.
- HENSEL, R. F. 1862. Über die Reste einiger Säugetierarten von Pikermi in der Münchener Sammlung. *Monatsberichte der Akademie der Wissenschaften*, **27**, 560–569.
- JANSSENS, L. A., VERHEIJEN, I. K., SERANGELI, J. and VAN KOLFSCHOTEN, T. 2019. Shoulder osteoarthritis in a European saber-toothed cat (*Homotherium latidens*) from the Lower Palaeolithic site of Schöningen (Germany). *International Journal of Paleopathology*, **24**, 279–285.
- JOJIĆ, V., BUGARSKI-STANOJEVIĆ, V., BLAGOJEVIĆ, J. and VUJOŠEVIĆ, M. 2014. Discrimination of the sibling species *Apodemus flavicollis* and *A. sylvaticus* (Rodentia, Muridae). *Zoologischer Anzeiger*, **253**, 261–269.
- JOLICOEUR, P. and MOSIMANN, J. E. 1960. Size and shape variation in the painted turtle. A principal component analysis. *Growth*, **24**, 339–354.
- KAUP, J. J. 1832. Vier neue Arten urweltlicher Raubthiere welche im zoologischen Museum zu Darmstadt aufbewahrt werden. *Archives für Mineralogie*, **5**, 150–158.
- KIFFNER, C. 2009. Coincidence or evidence: was the sabre-tooth cat *Smilodon* social? *Biology Letters*, **5**, 561–562.
- KOUFOS, G. D. 2016. Carnivora. *Geobios*, **49**, 53–67.
- KRETZOI, M. 1929. Materialien zur phylogenetischen Klassifikation der Aluroideen. *10th International Congress of Zoology, Budapest, 1927*, **2**, 1293–1355.
- LASCELLES, B. D. X., HANSEN, B. D., ROE, S., DEPUY, V., THOMSON, A., PIERCE, C. C., SMITH, E. S. and ROWINSKI, E. 2007. Evaluation of client-specific outcome measures and activity monitoring to measure pain relief in cats with osteoarthritis. *Journal of Veterinary Internal Medicine*, **21**, 410–416.
- LEIDY, J. 1853. Description of an extinct species of American lion: *Felix atrox*. *Transactions of the American Philosophical Society*, **10**, 319–321.
- LEIDY, J. 1868. Notice of some vertebrate remains from Hardin County, Texas. *Proceedings of the Academy of Natural Sciences of Philadelphia*, **20**, 174–176.
- LINNAEUS, C. 1758. *Systema naturae per regna tria naturae, secundum classis, ordines, genera, species cum characteribus, differentiis, synonymis, locis*, **1**, Tenth edition. Laurentii Salvii, Stockholm, Sweden.
- MADURELL-MALAPEIRA, J., RODRÍGUEZ-HIDALGO, A., AORAGHE, H., HADDOUMI, H., BARTOLINI LUCENTI, S., OUJAA, A., SALADIÉ, P., BENGAMRA, S., MARÍN, J., SOUHIR, M., FARKOUCH, M., MHAMDI, H., MAHDI AISSA, A., WERDELIN, W., CHACÓN, M. G. and SALA-RAMOS, R. 2021. First small-sized *Dinofelis*: evidence from the Plio-Pleistocene of North Africa. *Quaternary Science Reviews*, **265** (1), 107028.
- MARIANI, T. F. and ROMANO, P. S. 2017. Intra-specific variation and allometry of the skull of Late Cretaceous side-necked turtle *Bauruemys elegans* (Pleurodira, Podocnemididae) and how to deal with morphometric data in fossil vertebrates. *PeerJ*, **5**, e2890.
- MATTHEWS, T., DENYS, C. and PARKINGTON, J. E. 2007. Community evolution of Neogene micromammals from Langebaanweg ‘E’ Quarry and other west coast fossil sites, south-western Cape, South Africa. *Palaeogeography, Palaeoclimatology, Palaeoecology*, **245**, 332–352.
- MATTHEWS, T., VAN DIJK, E., ROBERTS, D. L. and SMITH, R. M. 2015. An early Pliocene (5.1 Ma) fossil frog community from Langebaanweg, south-western Cape, South Africa. *African Journal of Herpetology*, **64**, 39–53.
- McCALL, S., NAPLES, V. and MARTIN, L. 2003. Assessing behavior in extinct animals: was *Smilodon* social? *Brain, Behavior & Evolution*, **61**, 159–164.
- MEACHEN-SAMUELS, J. and VAN VALKENBURGH, B. 2009. Forelimb indicators of prey-size preference in the Felidae. *Journal of Morphology*, **270**, 729–744.
- MILLER, R. M., PICKFORD, M. and SENUT, B. 2010. The geology, palaeontology and evolution of the Etosha Pan, Namibia: implications for terminal Kalahari deposition. *South African Journal of Geology*, **113**, 307–334.
- MORALES, J., PICKFORD, M. and SORIA, D. 2005. Carnivores from the Late Miocene and Basal Pliocene of the Tugen Hills. *Kenya Revista de la Sociedad Geológica de España*, **18**, 39–61.
- MOSIMANN, J. E. and JAMES, F. C. 1979. New statistical methods for allometry with application to Florida red-winged blackbirds. *Evolution*, **33**, 444–459.
- NACARINO-MENESES, C. and CHINSAMY, A. 2021. Mineralized-tissue histology reveals protracted life history in the Pliocene three-toed horse from Langebaanweg (South Africa). *Zoological Journal of the Linnean Society*, **2021**, zlab037.
- PEIGNÉ, S., DE BONIS, L., LIKIUS, A., MACKAYE, H. T., VIGNAUD, P. and BRUNET, M. 2005. A new machairodontine (Carnivora, Felidae) from the Late Miocene hominid locality of Tm 266, Toros-Menalla, Chad. *Comptes Rendus Palevol*, **4**, 243–253.
- PICKFORD, M., SENUT, B., HIPODONKA, M., PERSON, A., SEGALÉN, L., PLET, C., JOUSSE, H., MEIN, P., GUERIN, C., MORALES, C. and MOURER-CHAUVIRE, C. 2009. Mio-Plio-Pleistocene geology and palaeobiology of Etosha Pan, Namibia. *Communications of the Geological Surveys of Namibia*, **14**, 95–139.
- POUDERS, C., DE MAESENEER, M., VAN ROY, P., GIELEN, J., GOOSSENS, A. and SHAHABPOUR, M. 2008. Prevalence and MRI-anatomic correlation of bone cysts in osteoarthritic knees. *American Journal of Roentgenology*, **190**, 17–21.

- ROBERTS, D. L. and BRINK, J. S. 2002. Dating and correlation of Neogene coastal deposits in the Western Cape (South Africa): implications for Neotectonism. *South African Journal of Geology*, **105**, 337–352.
- ROBERTS, D. L., MATTHEWS, T., HERRIES, A. I., BOULTER, C., SCOTT, L., DONDO, C., MTEMBI, P. and BROWNING, C. 2011. Regional and global context of the Late Cenozoic Langebaanweg (Lbw) palaeontological site: West Coast of South Africa. *Earth-Science Reviews*, **106**, 191–214.
- ROGERS, J. 1980. First report on the Cenozoic sediments between Cape Town and Eland's Bay. Geological Survey of South Africa, Report No. 1980-136, 136 pp.
- ROOK, L. and SARDELLA, R. 2008. An overview of the As Sahabi carnivore guild with description of new specimen from ELNRP field survey. 257–263. In BOAZ, N. T., EL-ARNAUTI, A., PAVLAKIS, P. and SALEM, M. J. (eds) *Circum-Mediterranean geology and biotic evolution during the Neogene Period: The perspective from Libya*. Garyounis Scientific Bulletin, Special Issue no. 5.
- ROTHSCHILD, B. M. and MARTIN, L. D. 2011. Pathology in saber-tooth cats. 35–42. In NAPLES, V. L., MARTIN, L. D. and BABIARZ, J. P. (eds) *The other saber-tooths: Scimitar-tooth cats of the western hemisphere*. Johns Hopkins University Press.
- ROUSSIAKIS, S. J. 2002. Musteloids and feloids (Mammalia, Carnivora) from the late Miocene locality of Pikermi (Attica, Greece). *Geobios*, **35**, 699–719.
- SALESA, M. J., ANTÓN, M., TURNER, A. and MORALES, J. 2006. Inferred behaviour and ecology of the primitive sabre-toothed cat *Paramachairodus ogygia* (Felidae, Machairodontinae) from the Late Miocene of Spain. *Journal of Zoology*, **268**, 243–254.
- SALESA, M. J., ANTÓN, M., SILICEO, G., PESQUERO, M. D. and ALCALÁ, L. 2014. First evidence of pathology in the forelimb of the Late Miocene saber-toothed felid *Promegantereon ogygia* (Machairodontinae, Smilodontini). *The Anatomical Record*, **297**, 1090–1095.
- SAMUELS, J. X., MEACHEN, J. A. and SAKAI, S. A. 2013. Postcranial morphology and the locomotor habits of living and extinct carnivorans. *Journal of Morphology*, **274**, 121–146.
- SAPOLSKY, R. M. 2004. Social status and health in humans and other animals. *Annual Review of Anthropology*, **33**, 393–418.
- SARDELLA, F. and WERDELIN, L. 2007. *Amphimachairodus* (Felidae, Mammalia) from Sahabi (latest Miocene–earliest Pliocene, Libya), with a review of African Miocene Machairodontinae. *Rivista Italiana di Paleontologia e Stratigrafia*, **113**, 67–77.
- SHAW, C. 1989. The collection of pathologic bones at the George C Page Museum, Rancho La Brea, California: a retrospective view. *Journal of Vertebrate Paleontology*, **9**(suppl. to no. 3), p. 38A.
- SHAW, C. A. and WARE, C. S. 2018. *Smilodon* paleopathology: a summary of research at Rancho La Brea. 196–206. In WERDELIN, L., MCDONALD, H. G. and SHAW, C. A. (eds) *Smilodon: The iconic sabertooth*. John Hopkins University Press.
- SHERMIS, S. 1983. Healed massive pelvic fracture in a *Smilodon* from Rancho La Brea. *PaleoBios*, **1**, 121–126.
- SLINGERLAND, L. I., HAZEWINKEL, H. A. W., MEIJ, B. P., PICAVET, P. and VOORHOUT, G. 2011. Cross-sectional study of the prevalence and clinical features of osteoarthritis in 100 cats. *The Veterinary Journal*, **187**, 304–309.
- SMITH, R. and HAARHOFF, P. 2006. Sedimentology and taphonomy of an early Pliocene Sivathere Bonebed at Langebaanweg, Western Cape Province, South Africa. *African Natural History*, **2**, 197–198.
- TURNER, A. 1997. *The big cats and their fossil relatives: An illustrated guide to their evolution and natural history*. Columbia University Press.
- VALENCIANO, A. and BASKIN, J. 2022. *Moralesictis intrepidus* gen. et sp. nov., the long journey of a Miocene honey badger's relative to the New World. *Historical Biology*, **34**, 1413–1422.
- VALENCIANO, A. and GOVENDER, R. 2020a. New insights into the giant mustelids (Mammalia Carnivora, Mustelidae) from Langebaanweg fossil site (West Coast Fossil Park, South Africa, early Pliocene). *PeerJ*, **8**, e9221.
- VALENCIANO, A. and GOVENDER, R. 2020b. New fossils of *Mellivora benfieldi* (Mammalia, Carnivora, Mustelidae) from Langebaanweg 'E' Quarry (South Africa, early Pliocene): re-evaluation of the African Neogene mellivorines. *Journal of Vertebrate Paleontology*, **40**, e1817754.
- VALENCIANO, A., MORALES, J. and GOVENDER, R. 2022. *Eucyon khoikhoi* sp. nov. (Carnivora, Canidae) from Langebaanweg 'E' Quarry (early Pliocene, South Africa): the most complete African canini from the Mio-Pliocene. *Zoological Journal of the Linnean Society*, **194**, 366–394.
- VAN DIJK, D. E. 2003. Pliocene frogs from Langebaanweg, Western Cape Province, South Africa. *South African Journal of Science*, **99**, 123–124.
- VANN, S. and THOMAS, R. 2006. Humans, other animals and disease: a comparative approach towards the development of a standardised recording protocol for animal palaeopathology. *Internet Archaeology*, **20**. <https://doi.org/10.11141/ia.20.5>
- VERRUIJT, M. J. 2009. Prevalence of osteoarthritis in the joints of the appendicular skeleton of the cat. PhD thesis. Utrecht University, Faculty of Veterinary Medicine, Netherlands. <https://studenttheses.uu.nl/handle/20.500.12932/2363>
- VIRET, J. 1939. Monographie paléontologique de la faune de vertébrés des sables de Montpellier. III. Carnivora Fissipedia. *Travaux du Laboratoire de Géologie de la Faculté de Sciences de Lyon*, **37**, 7–26.
- WAIBL, H., GASSE, H., HASHIMOTO, Y., BURDAS, K. D., CONSTANTIN-NESCU, G. M., SABER, A. S., SIMOENS, P., SALAZAR, I., SOTONYI, P., AUGSBURGER, H. and BRAGULLA, H. 2005. *Nomina anatomica veterinaria*, Fifth edition. International Committee on Veterinary Gross Anatomical Nomenclature. World Association of Veterinary Anatomists, Hanover, Germany.
- WALDRON, T. 2009. *Palaeopathology*. Cambridge University Press.
- WERDELIN, L. 2003. Mio-Pliocene Carnivora from Lothagam, Kenya. 261–330. In LEAKEY, M. and HARRIS, J.

- (eds) *Lothagam: The dawn of humanity in Eastern Africa*. Columbia University Press.
- WERDELIN, L. 2006. The position of Langebaanweg in the evolution of Carnivora in Africa. *African Natural History*, **2**, 201–202.
- WERDELIN, L. and LEWIS, M. E. 2001. A revision of the genus *Dinofelis* (Mammalia, Felidae). *Zoological Journal of the Linnean Society*, **132**, 147–258.
- WERDELIN, L. and PEIGNÉ, S. 2010. Carnivora. 603–657. In WERDELIN, L. and SANDERS, W. (eds) *Cenozoic mammals of Africa*. University of California Press.
- WERDELIN, L. and SARDELLA, R. 2006. The *Homotherium* from Langebaanweg, South Africa and the origin of *Homotherium*. *Palaeontographica Abteilung A*, **227**, 123–130.
- WERDELIN, L., TURNER, A. and SOLOUNIAS, N. 1994. Studies of fossil hyaenids: the genera *Hyaenictis* Gaudry and *Chasmaporthetes* Hay, with a reconsideration of the Hyaenidae of Langebaanweg, South Africa. *Zoological Journal of the Linnean Society*, **111**, 197–217.
- ZDANSKY, O. 1924. Jungtertiäre Carnivoren Chinas. *Palaeontologia Sinica Series*, **2**, 1–149.